Mineral formation at the PT-parameters

Bobrov A.V.[1], Litvin Yu.A.[2], Ismailova L.S.[1]

Diamond-forming efficiency of chloride-silicate-carbonate melts

1-Geol. dep. MSU; [2]-IEM RAS *archi3@yandex.ru*

Keywords: diamond synthesis, carbonatite, chloride, eclogite

According to the carbonatite model of the diamond formation [Litvin, 2007] based on the large volume of mineralogical and physicochemical experimental information, carbon-silicate-carbonate (carbonatitic) melts with widely variable compositions are the growth medium for most mantle diamonds and inclusions in them. In addition to the major completely miscible carbonate and silicate components (minerals of peridotite and eclogite assemblages), such melts contain minor soluble components (oxides, phosphates, chlorides, C-O-H-N fluids, and others), as well as minor completely immiscible and insoluble solid and melt phases (sulfides, metals). The diamond-forming efficiency of silicate-carbonate melts clearly corresponds to the important criterion of syngenesis of diamond with its silicate and carbonate inclusions. High-pressure experimental associations not only comprise the whole set of minerals typical for inclusions in diamonds of peridotitic (olivine, garnet, clino-, and orthopyroxenes) and eclogitic (garnet and clinopyroxene) type, but demonstrate the characteristic features of minerals of diamond paragenesis. These comprise significant admixtures of Na in garnets and K in clinopyroxenes, which are the reliable indicators of crystallization of these minerals from alkaline silicate-carbonate melts.

Experimental investigations of multicomponent peridotite-carbonatite and eclogite-carbonatite systems at a standardized pressure of 8.5 GPa within the narrow pressure range of 1760-1820°C demonstrated that the diamond-forming efficiency of their carbon-bearing melts had concentration limitations [Bobrov and Litvin, 2009]. The compositions effective for the diamond nucleation comprise only significantly carbonatite parts of the systems and are limited by the concentration barriers of diamond nucleation (CBDN) in the cases of K-Na-Ca-Mg-Fe-carbonatite, Ca-Mg-, and K-carbonate compositions (at the concentrations of 30, 25, and 30 wt % of peridotite components and 35, 30, and 45 wt % of eclogite component, respectively). This means that the inhibitory influence of peridotite and eclogite components dissolved in carbon-bearing carbonatite melts on diamond nucleation is observed only at their relatively low concentrations.

We established the diamond-forming efficiency of chloride [Litvin, 2003] and chloride-carbonate [Tomlinson et al., 2004] melts with dissolved carbon. The concentration of chloride components in some fluid/melt inclusions in diamonds is quite significant [Izraeli et al., 2001; Klein-BenDavid et al., 2004]. As this takes place, their influence on the diamond formation (and mainly on CBDN position) in multicomponent silicate-carbonate melts is not clear and requires experimental investigation. In this study we performed testing of the diamond-forming efficiency of chloride-silicate-carbonate melts with dissolved carbon, the components of which are widely abundant in crystal and fluid/melt inclusions in natural diamonds. The silicate component is represented by the model compositions of bimineral eclogite; the carbonate component, by multicomponent K-Mg-Ca-carbonatite; chloride component, by mixture of KCl and NaCl taken in equal weight proportions. 40 wt % of chemically pure graphite was added to the prepared chloride-silicate-carbonate mixtures.

Our investigations were performed on a high-pressure toroidal "anvil-with-hole" apparatus using special cells with tubular graphite heaters [Bobrov and Litvin, 2009] at standardized PT-parameters (8.5 GPa, 1800°C) in the Institute of Experimental Mineralogy, Russian Academy of Sciences. We performed two series of experiments. The first series was carried out in the carbonate-silicate system in order to determine the compositional range (the relationships between silicate and carbonate components, CBDN), in which spontaneous nucleation occurs during the first minutes of the experiment; the run duration did not exceed 10 min. The second experimental series was aimed on the study of the influence of chloride components on diamond crystallization in multicomponent melts.

The first series of experiments allowed us to observe the formation of graphite (the area of metastable oversaturation) or diamond (the area of labile solutions) depending on relationships between silicates and carbonates. In the first case small segregations of graphite as scales or round globules were obtained. As this took place, the growth of diamond was registered on (100) and (111) seed faces. In the second case we obtained diamond as octahedral and twins (spinel law). We calculated the density of diamond nucleation, which characterizes the number of embryos in the volume unit of experimental samples and, accordingly, may be the quantitative characteristic of the diamond-forming efficiency. The values obtained (from $4.1*10^4$ to $6.7*10^4$ grains/mm^3) are quite high being typical for diamond synthesis in carbonate melts. Spontaneous diamond nucleation was obtained for the compositions $(Ecl_{20}Carb_{80})_{60}C_{40}$ and $(Ecl_{30}Carb_{70})_{60}C_{40}$. The latter composition was accepted as the CBDN position; because of this, it was applied in the second experimental series.

In the second experimental series performed with participation of chloride components, the formation of diamond was registered only for two starting compositions ($[Ecl_{21}Carb_{49}Chl_{30}]_{60}C_{40}$ and $[(Ecl_{15}Carb_{62})Chl_{23}]_{60}C_{40}$), the density of nucleation decreased ($2.2*10^4$ grains/mm^3), whereas average crystal sizes increased. Note that the relationships between carbonate and silicate components in the first composition correspond to the CBDN of chloride-free carbonate-silicate melts obtained in the first series. Increase of chloride concentration in comparison with this composition $[(Ecl_{20}Carb_{47})Chl_{33}]_{60}C_{40}$ results in termination of diamond spontaneous nucleation. Some runs performed at long durations demonstrated the samples with clear signs of liquid immiscibility [Safonov et al., 2007]: globules of essentially chloride composition (SiO_2 1.13; Al_2O_3 0.43; FeO 1.87; MgO 7.58; CaO 9.64; Na_2O 13.58; K_2O 30.36; Cl 32.98 wt %) are located in the silicate-carbonate groundmass (SiO_2 4.31; Al_2O_3 0.77;

FeO 0.85; MgO 41.69; CaO 18.84; Na_2O 2.46; K_2O 2.23; Cl 2.57 wt %). As this took place, the formation of diamond occurred only in silicate-carbonate (carbonatite) melt. In our opinion, this observation, as well as termination of spontaneous diamond nucleation with increase of chloride concentration provides evidence for the negative influence of chloride components on the diamond formation, at least in the cases of their high concentrations.

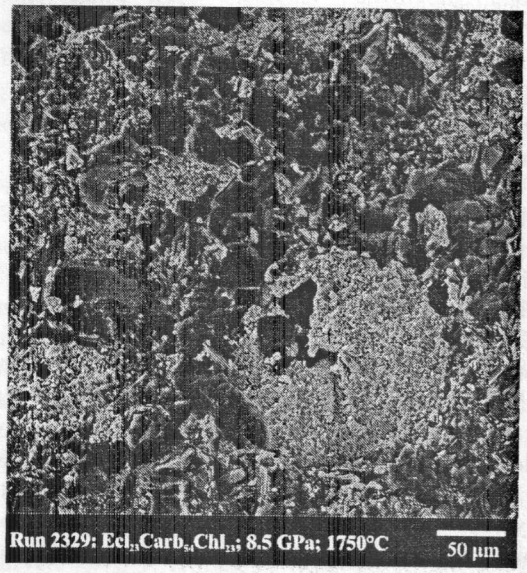

Fig. 1. Effect of immiscibility between chloride and silicate-carbonate melts in the experimental sample after quenching. Diamond crystals occur in fine-granular silicate-carbonate groundmass. Secondary electron image.

The study was supported by the Russian Foundation for Basic Research (project nos. 09-05-00027 and 11-05-00401), and grants of the President of Russian Federation for the state support of the young Russian scientists (MD-534.2011.5) and leading scientific schools (NSh-3634.2010.5).

References

1. Bobrov A.V., Litvin Yu.A. (2009) Peridotite-eclogite-carbonatite systems at 7.0-8.5 GPa: concentration barrier of diamond nucleation and syngenesis of its silicate and carbonate inclusions, *Rus. Geol. Geophys. 50.* 1221–1233.
2. Litvin Yu.A. (2003) Alkaline-chloride components in the processes of diamond growth under mantle conditions and conditions of high pressure experiment. Dokl. Earth Sci. 389A, 388-391.
3. Izraeli E.S., Harris J.W., Navon O. (2001) Brine inclusions in diamonds: a new upper mantle fluid, *Earth Planet. Sci. Lett. 187.* 323–332.
4. Klein-BenDavid O., Izraeli E.S., Hauri E., Navon O. (2004) Mantle fluid evolution – a tale of one diamond, *Lithos. 77.* 243–253.
5. Litvin Yu.A. (2007) High-pressure mineralogy of diamond genesis / In: Advances in high-pressure mineralogy (ed. Ohtani E.), Geol. Soc. Amer. Spec. Pap. *421.* 83–103.
6. Safonov O.G., Perchuk L.L., Litvin Yu.A. (2007) Melting relations in the chloride-carbonate-silicate systems at high-pressure and the model for formation of alkalic diamond-forming liquids in the upper mantle, *Earth Planet. Sci. Lett. 253.* 112–128.
7. Tomlinson E., Jones A., Milledge J. (2004) High-pressure experimental growth of diamond using C–K_2CO_3–KCl as an analogue for Cl-bearing carbonate fluid, *Lithos. 77.* 287–294

Kuzyura A.V.[1], Litvin Yu.A.[1], Okoemova V.Yu.[2], Vasiliev P.G.[2], Wall F.[3], Jeffries T.[4] Experimental study of interphase partitioning of rare elements in diamond forming eclogite-carbonatite and peridotite-carbonatite systems

[1] IEM RAS; [2] Geol. Dep. MSU; [3] Cornwall Campus of University of Exeter, UK; [4] Natural History Museum, UK
shushkanova@iem.ac.ru fax(496)5249687 ph. (496)5225876

Study of geochemistry of syngenetic inclusions with growth carbonate-silicate melts and minerals that crystallized together with diamond in them are complicated, and data about trace elements partitioning numbers between mineral and melt phases of diamond forming systems of the Earth mantle are extremely low.

Earlier authors studied at high pressure phase relations and interphase participation of rare elements at melting of natural carbonatite [*Kuzyura et al*, 2008]. Possible compositions of chemically changeable carbonate-silicate growth medium for diamond were modeled by mafic carbonatite from Chagatai complex (Uzbekistan). Their melts are highly effective for diamond nucleation [*Litvin et al*, 2001, 2005]. At that time garnets and clinopyroxenes similar to ones associating with high calcic diamondiferous eclogites and grosspidites form syngenetically with diamonds. [*Bobrov et al*, 2004].

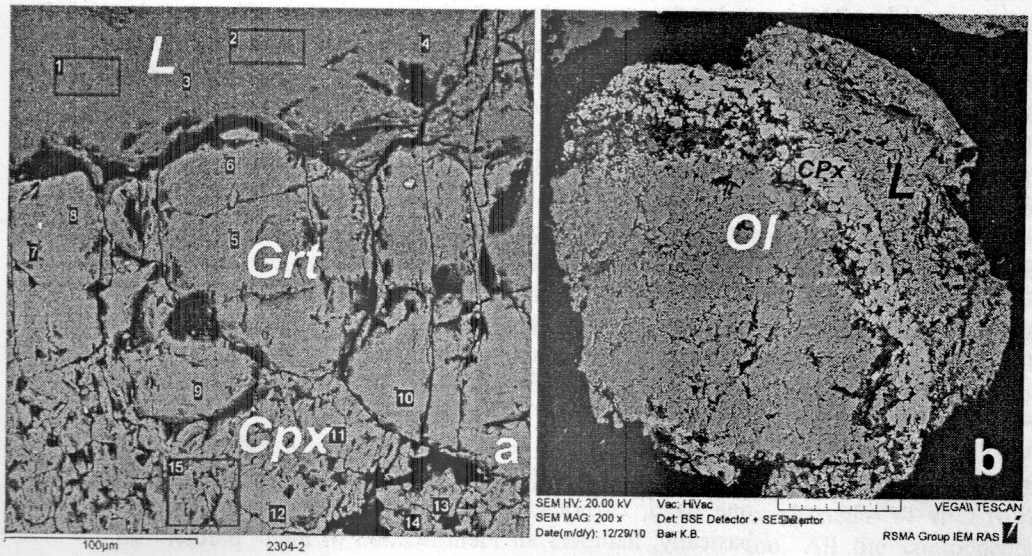

Fig. 1. SEM photograph of experimental samples: a) sample 2304, system eclogite-carbonatite $[CPx_{52}Grt_{28}(SiO_2)_{20}]_{59.3}Dol_{39.3}RE_{1.4}$, 8.5 GPa, 1600°C, duration 155 min; b) sample 2351, system peridotite-carbonatite $[Per_{30}Carb_{70}]_{99}RE_1$, 7 GPa, 1400°C, duration 180 min. Grt – garnet, CPx – clinopyroxene, Ol – olivine, L – completely miscible carbonate-silicate melt, Dol – dolomite, RE – mixture of rare elements, Per – peridotite, Carb – carbonate

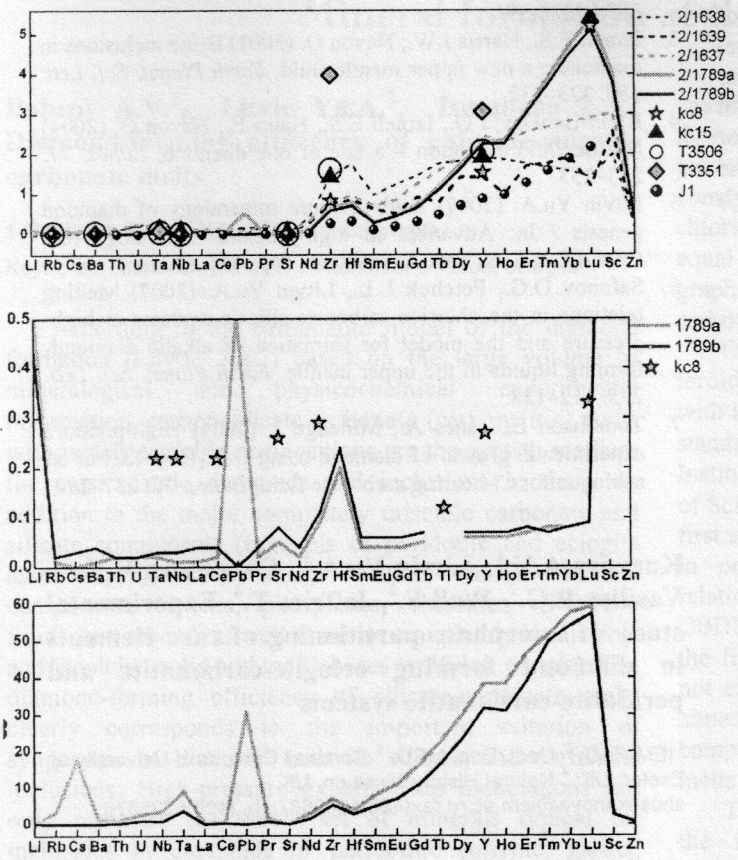

Fig. 2. Diagrams of interphase participation of rare elements between: (a) – garnet and carbonate-silicate melt; (b) – clinopyroxene and carbonate-siflicate melt; (c) – garnet and clinopyroxene; kc8, kc15, T3506, T3351, J1-data from literature; 2/1638, 2/1639, 2/1637, 2/1789 – our experimental samples obtained at melting of natural Chagatai carbonatite and model system eclogite-carbonatite.

Further study of participation of rare elements in diamondiferous mantle systems was relates to model eclogite-carbonatite and peridotite-carbonatite systems. In this connection series of experiments on experimental research of equilibrium participation of rare elements "mineral-melt" and "mineral-mineral" in eclogite-carbonatite and peridotite-carbonatite systems were carried out with using of apparatus "anvil-with-hole"-like (IEM RAS) at 7-8.5 GPa. Prepared in special way mixture of rare elements, mainly in oxides: Li, Rb, Cs, Ba, Th, U, Ta, Nb, La, Ce, Pb, Pr, Sr, Nd, Zr, Hf, Sm, Eu, Gd, Tb, Dy, Y, Ho, Er, Tm, Yb, Lu, Sc, и Zn was added to the systems. Starting proportions of components were $[[CPx_{40\text{-}64}Grt_{16\text{-}40}(SiO_2)_{20}]_{59.3}Carb_{39.3}]_{98.6}RE_{1.4}$ for eclogite-carbonatite system and $[[Ol_{36\text{-}60}OPx_{16}CPx_{12\text{-}24}Grt_{12\text{-}24}]_{30}Carb_{70}]_{99}RE_1$ for peridotite-carbonatite system. After quenching experimental samples were spited and polished. Electron microprobe and SEM researches were carried out on the polished surfaces with carbon covering in IEM RAS. Contents of trace elements in grains on the same samples (carbon covering has been removed from) were determined using of method of LA-ICP-MS in mineralogical department of the London Natural History Museum.

We analyzed homogeneous melt areas and isometric grains of minerals – garnet, clinopyroxene, olivine.

Quite large (more than 100 *μm*) garnet, clinopyroxene, and olivine crystals crystallized form melt in experiments at 7.0 – 8.5 GPa (fig. 1). Mostly the crystals appear surrounded by melt in quenched samples. In some cases large crystals are separated from parental carbonate-silicate quenched melt because of low viscosity of the melt and gravitation. Carbonate-silicate melt is in intergranular space in such samples. Melt of model eclogite-carbonatite and peridotite-carbonatite systems quenches as cryptocrystalline aggregate. Most cryptocrystalline areas were chosen for analyses, analyses was done on squares.

Based on results of analyses of content of rare elements in experimental phases by LA-ICP-MS-method, coefficients of interphase participation (Kd) garnet-melt, clinopyroxene-melt, and garnet-clinopyroxene were calculated. There is a diagram demonstrating participation of rare elements between garnet and carbonate-silicate melt, clinopyroxene and carbonate-silicate melt, and garnet and clinopyroxene on Fig. 2. Such kind of data present for natural system with Chagatai carbonatite and for model eclogite-carbonatite system only. The main feature of the obtained picture of interphase partitioning of trace elements is quite different behavior of light (La, Ce, Pr) in relation to medium and heavy (Nd, Zr, Hf, Sm, Eu, Gd, Tb, Dy, Y, Ho, Er, Tm, Yb, Lu) rare-earth elements. While light elements are mainly distributed in melt phase, the heavy ones go to garnet. A number of elements including LILE (Rb, Sr, Ba), Sc, as well as Zn, Ta, Pb, Th, and U Sc, V, Y, Zr, and Hf have a clearly expressed affinity to carbonate-silicate melt. A curve format on the diagram of participation garnet-melt is practically confirms a curve format for garnet-clinopyroxene participation, this testifies to that main participants of rare elements distribution are garnet and carbonate-silicate melt, clinopyroxene plays a part of Zn-concentrator in the process.

By preliminary data, garnet and clinopyroxene are main collectors of rare elements in peridotite-carbonatite system.

The obtained participation pictures were compared with data of different researchers. Experimental study of interphase partitioning of trace elements between garnet and carbonatite melts and other chemically different melts were spent before for limited set of rare elements at 2.7 – 3.3 GPa and 1000°C (*Sweeney et al.*, 1992, 1995; *van Westrenen et al*, 1999; *Walter et al*, 2008). However those used PT -parameters were not within the area of thermodynamic stability of diamond. For comparison Kd available from literature on these researches were inserted on our graphs of participation. Thus, there were find out a similarity in contrast behavior of light and heavy REE and other RE at comparison of distribution of rare elements between garnet and carbonate-silicate melt of Chagatai carbonatite and model eclogite-carbonatite system, from one side, and garnet and model silicate melt, from other side *(van Westernen et al*, 1999).

Therefore, the detected similarity in tendencies of trace elements partitioning between garnet phase, on the one hand, carbonatite and silicate melts, with another, basically, hampers an identification of melt "partner" on

the basis of relative contents of trace elements for garnet phase only

The results demonstrate that rare elements participation doesn't depend significantly on melt composition. Heavy RE are concentrated in a melt. Diamondiferous carbonate-silicate, carbonate, and silicate melts behave similarly in respect of participation of rare elements.

Data about trace elements partitioning numbers between mineral and melt phases of diamond forming systems of the Earth mantle were unknown until the present work. Studying of interphase trace elements partitioning patterns for mantle diamond forming processes becomes possible in connection with development of methods of physical and chemical experiment together with high-sensitivity analytical methods. These investigations have also more general geochemical value as formation of growth media for a great bulk of natural diamonds and syngenetical minerals included in them are a part of general process of magmatic evolution of mantle substances and is integrated physico-chemically and spatially to it.

Financial support: RFBR 10-05-00654, 11-05-0040, grant of The President RF № MK- 913.2011.5

References

1. Kuzyura A.V., T. Jeffries, F. Wall, Yu. A. Litvin (2008), Partitioning of trace elements between garnet, clinopyroxene and diamond-forming carbonate-silicate melt at 7 GPa, *Mineralogical Magazine*, Vol. 74, № 2, pp. 227–239
2. Litvin Yu.A., A.P. Jones, A.D. Berd et al. (2001), Crystallization of diamond and syngenetic minerals in melts of diamondiferous carbonatites of the Chagatai Massif, Uzbekistan: Experiment at 7.0 GPa, *Doclady Earth Sciences*, V. 381, № 9, pp. 1066-1069
3. Litivn Yu.A., G.Kurat, G.Dobosi (2005), Experimental study of diamondite formation in carbonate-silicate melts: a model approach to natural processes, *Russian Geology and Geophysics*, V. 46, № 12, pp. 1285-1300
4. Bobrov A.V., Yu.A.Litivn, F.K.Divaev (2004), Phase relations and diamond synthesis in the carbonate-silicate rocks of the Chagatai Complex, Western Uzbekistan: Results of experiments at P=4-7 GPa and T=1200-1700 degrees C, *Geochemistry International*, V. 42, № 1, pp. 39-48
5. Sweeney R.J., D.H. Green, S.H. Sie (1992), Trace and minor element partitioning between garnet and amphibole and carbonatitic melt, *Earth and Planetary Science Letters*, V. 114, № 1-2, pp.1-14
6. Sweeney R.J., V. Prozesky, W. Przybylowich (1995) Selected trace and minor element partitioning between peridotite minerals and carbonatite melts at 18-46 kb pressure, *Geochimica et Cosmochimica Acta*, V. 59, pp. 3671-3683
7. Van Westrenen W., J. Blundy, B. Wood (1999) Crystal-chemical controls of trace element partitioning between garnet and anhydrous silicate melt, *American Mineralogist*, V. 84, pp. 838-847
8. Walter M.J., G.P. Bulanova, L.S. Armstrong , et al (2008), Primary carbonatite melt from deeply subducted oceanic crust, *Nature*, V. 454, pp. 622-626

Litvin Yu.A.[1], Vasiliev P.G.[2], Bobrov A.V.[2], Okoyomova V.Yu.[2], Kuzyura A.V.[1] Parental media for diamonds and primary inclusions by evidence of physicochemical experiment

[1] *IEM RAS;* [2] *Geol. dep. MSU* litvin@iem.ac.ru fax (496) 52496 87 ph: (496) 522 58 76

Key words: diamond, diagram of parental medium, primary inclusions, experiment, syngenesis diagram, classification of inclusions

Abstract The mantle-carbonatite conception of genesis of diamond (Litvin, 2007, 2009) is briefly outlined. A generalized diagram of compositions of the multi-component heterogeneous parental medium for diamond and primary inclusions therein is first developed. Boundary compositions of the parental medium diagram are represented by mineral components of the peridotitic and eclogitic parageneses, mantle carbonatites and C-O-H-fluids, phases of accessory type both soluble in the carbonate-silicate melts (chlorides, phosphates, etc.) and insoluble in them (sulfides), as well as carbon. Phase relations of the multi-component eclogite-carbonatite-sulfide-diamond are studied at 7 GPa. "Syngenesis diagram" for diamond, paragenetic and xenogenetic minerals (including the solubility curves of diamond in carbonate-silicate and sulfide melts) is constructed. Physicochemical mechanism of formation of diamond and paragenetic minerals is revealed. Genetic classification of primary inclusions in natural diamonds is worked out. Analysis of physicochemical history of diamond formation in the mantle chamber of carbonatite magma is accomplished.

Introduction The mantle-carbonatite conception of genesis of diamond of kimberlite deposits (Litvin, 2007[a, b], 2009) is justified by the complex of mineralogical, experimental and theoretical data. Completely miscible carbonate-silicate growth melts with dissolved elemental carbon (carbon source for diamond) form a basis for the parental media for the dominating mass of natural diamonds and paragenetic minerals. The parental carbonate-silicate-carbon melts are multi-component heterogeneous media with strongly changeable compositions. So, silicate constituents are presented by minerals and components both peridotite and eclogite parageneses (Sobolev, 1974). It is established in the high-pressure high-temperature experiments that both peridotite-carbonatite-carbon and eclogite-carbonatite-carbon melts are represented as highly efficient diamond-forming media. An example of diamond crystallization in melt oversaturated in dissolved carbon of the eclogite-carbonatite system is demonstrated in the fig. 1.

Composition diagram of parental medium for diamond and primary inclusions. A generalized diagram of compositions of the multi-component heterogeneous parental medium for diamond and primary inclusions therein is developed (Fig. 2). The major composition tetrahedron of the system "peridotite-eclogite-carbonatite-soluble admixture componens" is its basic element. Belonging of the mineral assemblage of syngenetic inclusions in natural diamonds to two major parageneses, - peridotitic and eclogitic, - is took into consideration. The boundary compositions of the parental medium diagram are determined with mineral components of the auxiliary tetrahedrons – peridotitic (Ol-Opx-Cpx-Grt), eclogitic (Cpx-Grt-Crn-Coes), mantle carbonatite (Mg, Fe, Ca, K, Na, etc. carbonates), phases and components of admixtured accessory sort – soluble in carbonate-silicate melts (chlorides, phosphates, etc.) including the components of C-O-H-volatile compounds, and carbon too. All the components of the boundary tetrahedrons

mentioned above are responsible for formation of paragenetic mineral phases together with diamond and, correspondingly, for capture of the paragenetic inclusions by natural diamonds. At the same time due to physicochemical experiment it turned out that xenogenetic mineral phases are presented within the assemblage of so called syngenetic inclusions. Sulfide minerals which are not soluble in diamond-forming carbonate-silicate melts as well as sulfide melts which are completely immiscible with these are among the xenogenetic phases. In the fig. 2, the auxiliary boundary tetrahedron for sulfide components is positioned out of the major tetrahedron and is divided by conventional boundary c. l. i. b. (complete liquid immiscibility boundary). This boundary symbolizes xenogenetic nature of sulfides in diamond-forming carbonate-silicate growth media.

Fig. 1

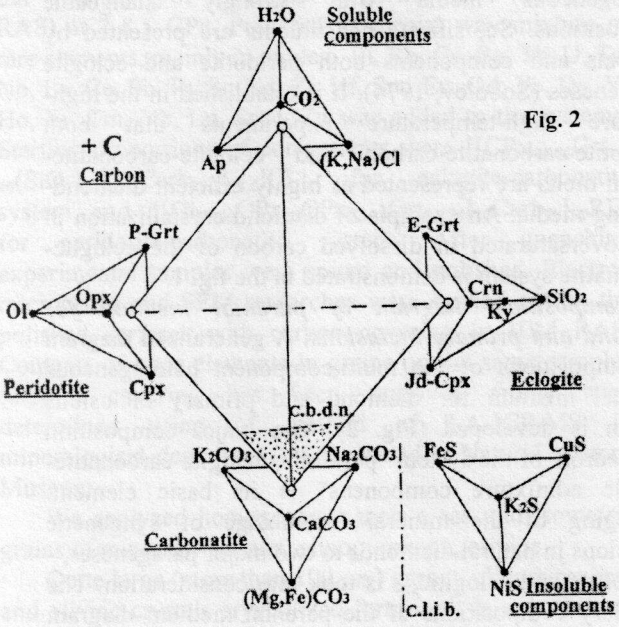

Fig. 2

The compositions of diamond-forming parental media belongs to carbonatites by experimental estimation ov concentration barriers of diamond nucleation, that is limiting for diamond formation compositions in peridotite-carbonatite (30 wt.% peridotite) and eclogite-carbonatite (35 wt.%eclogite) systems (Litvin et al., 2008; Bobrov, Litvin, 2009). By doing so it has been ascertained that compositions of the peridotite-carbonatite and eclogite-carbonatite growth melts are fell within the carbonatite concentration interval. Primary hermetically included minerals, melts and C-O-H-fluid components in natural diamonds arethe fragments of the parental medium which are captured *in situ* by growing diamonds.

Syngenesis diagram for the eclogite-carbonatite-sulfide-diamond system .Under the pressure of 7 GPa (diamond thermodynamic stability conditions), melting phase relations of the multi-component heterogeneous system eclogite-carbonatite-sulfide-diamond are experimentally studied. Composition of the system brings into proximity with the parental medium udner conditions of eclogite paragenesis. A "syngenesis diagram" for diamond, paragenetic and xenogenetic minerals (in respect to diamond) which are presenting at the parental medium is constructed (Fig. 3). Within the diagram, the syngenesis diagram for diamond and paragenetic inclusions in the system eclogite-carbonatite-diamond (solid lines) and phase relation diagram for the "xenogenetic" system sulfide-diamond (dashed lines) are combined with the use of the projection method. This makes it possible to obtain a common picture of phase relations in multi-component heterogeneous diamond-forming medium as well as a notion of conditions for joint capture of paragenetic and xenogenetic phases by growing diamonds. For detailed information see (Litvin et al., 2011). New physicochemical results including diamond solubility curves in completely miscible carbonate-silicate (20-22 wt. % carbon) and sulfide (30-32 wt. % carbon) melts and the solubility curves relationships with the boundaries of phase regions for carbonate-silicate and sulfide phases are obtained. The syngenesis diagram gives opportunity to reveal clearly the physicochemical mechanisms of formation of natural diamond and paragenetic minerals. This permits to determine formation conditions of the silicate and carbonate minerals paragenetic in respect to diamond. Also, conditions of coexistence of xenogenetic sulfide minerals and melts with the paragenetic phases are determined. Thereby, physicochemical conditions of *in situ* trapping by growing diamonds of paragenetic and xenogenetic minerals and melts (known in mineralogy of diamond genesis as "syngenetic" or "primary" inclusions) are cleared up. The experimental results and conclusions are essentially important for justification of the mantle-carbonatite conception of diamond genesis (Litvin, 2007, 2009).

Genetic classification of primary inclusions in natural diamond. The data of analytical mineralogy of inclusions and physicochemical experiment, if generalized, allows to work out a genetic classification of primary inclusions in natural diamonds. The classification reveals origin of the inclusions, their physicochemical links with the major components of carbonate-silicate growth melts as well as with soluble and insoluble components and phases containing by the growth melts (Litvin, 2009). By physicochemical conditions of their origin, the primary inclusions in diamonds could be related to the next groups: (1) major silicate, aluminosilicate, carbonate components and dissolved carbon which are responsible for paragenetic inclusions of Mg-Fe-Ca-silicates, Na-K-Mg-Ca-Fe-aluminosilicates, Mg-Ca-Fe-Al-Si-oxides, Mg-Ca-Fe-Na-K-carbonates, multi-component carbonatite melts, diamond, and unstable graphite; (2) secondary soluble admixtured components – oxides,

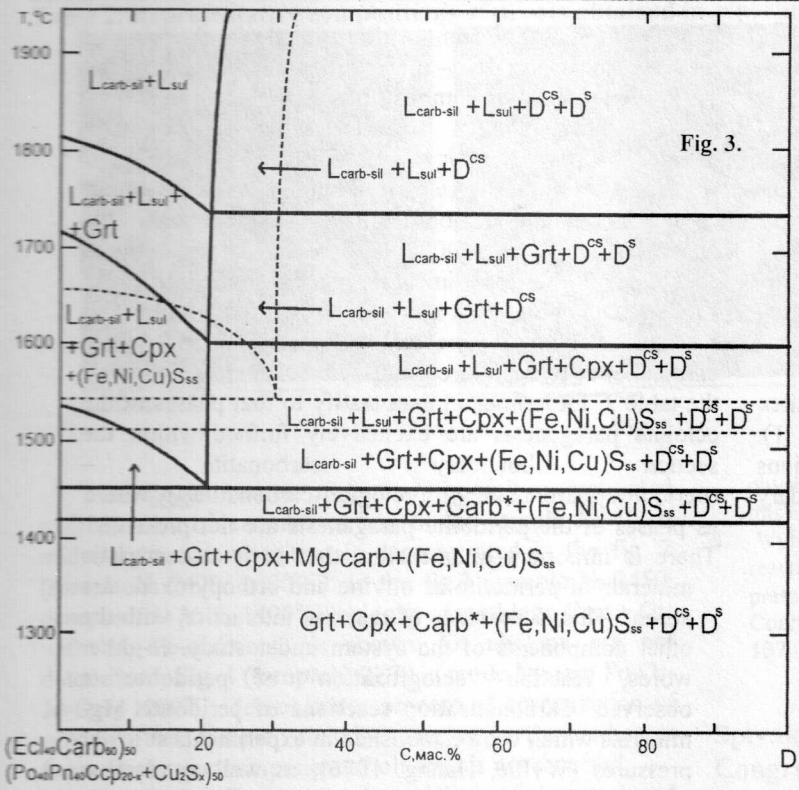

Fig. 3.

accessory silicates and aluminosilicates, phosphates, chlorides which are responsible for formation of paragenetic minor phases; (3) secondary soluble admixtured components of the C-O-H system which are responsible for formation of paragenetic phases of volatile compounds (H_2O, CO_2, etc.) released under solidification of growth melt; (4) secondary phases insoluble and completely immiscible if liquid with carbonatite melts which are responsible for capture of xenogenic sulfides, native metals, etc.

Physicochemical evolution of natural diamond-forming chamber The syngenesis phase diagram for diamond, paragenetic and xenogenetic minerals and melts allows to consider a physicochemical history of diamond formation in the mantle chamber of carbonatite magma (Litvin, 2009) and to approach an estimation of the conditions of their origin in the substance of the Earth's peridotite mantle.

The study is supported by the next grants – of the RF President MD-534.2011.5, RFBR 09-05-00027, 10-05-00654, 11-05-00401; НШ-3654-2010.

References

1. Bobrov A.V., LitvinYu.A. (2009), Pridotite-eclogite-carbonatite systems at 7.0 – 8.5 GPa: Concentration barrier of diamond nucleation and syngenesis of its silicate and carbonate inclusions, *Russian Geology and Geophysics*, Vol. 50, № 12, pp. 1188-1200.
2. LitvinYu.A. (2007[a]), High-pressure mineralogy of diamond genesis.Advances in High-Pressure Mineralogy (Ohtani E., ed.): Geological Society of America Special Paper 421, pp. 83-103.
3. LitvinYu.A.(2007[b]), Experiment in solution of the problem of diamond genesis, Zapiskiof the Russian Mineralogical Society, Vol. 136, № 7, pp. 138-158.
4. LitvinYu.A. (2009), The physicochemical conditions of diamond formation in the mantle matter: experimental studies, Russian Geology and Geophysics, Vol. 50, № 12, pp. 1188-1200.
5. LitvinYu.A., LitvinV.Yu., Kadik A.A.(2008), Diamond crystallization in melts of mantle silicate-carbonate-carbon systems, from experimental data obtained at 7.0 – 8.5 GPa, Geochemistry International, , № 6.
6. SobolevN.V. (1977), Deep-Seated Inclusions in Kimberlites and the Problem of the Composition of the Upper Mantle, Am. Geophys. Union, Washington, 304 p.

Pokrovskaya N.E.[1], LitvinYu.A.[2] Experimental modeling of syngenesis of diamond and minerals of peridotite and eclogite parageneses

[1] Geol. dep. MSU; [2] IEM RAS for_nataliya@list.ru
fax (496)5249687 ph (496)5225876

Key words: diamond, parental media, paragenetic inclusions, experiment, eclogitization of peridotite minerals

Abstract Study of physicochemical conditions of syngenesis of diamond and mineral phases of peridotite and eclogite paragenese sin changeable carbonatite parental media is started at 8 GPa and 1200 – 1800oC. Experimental determinations testify that the compositions of parent media for diamond and inclusins belog to the phase field "boundary carbonatite- peridotite30carbonatite70 - eclogite35carbonatite65". It is found that the processes of olivine carbonatization as well as garnetization while it reacts with jadeite component are developed at regions of complete and partial melting of the compositions rich in peridotite constituents. As the result of the processes, the stability region for the minerals of peridotite paragenesis is contracted, but that is extended in the case of eclogite paragenesis.

Introduction Analytical mineralogy of primary ("syngenetic") inclusions is the only plausible source of information on chemical composition of the parental media for natural diamonds and phases trapped by these while growing. Along with this, physicochemical experiment permits to obtain the objective information on genetic links of diamond and phases included therein. It becomes possible if the diamond-forming systems which boundary compositions are chosen to take into account the evidence of the inclusions mineralogy. The mantle-carbonatite theory of diamond genesis (Litvin, 2007, 2009) is developed as a result of generalization of mineralogical and experimental data that sort of. According to the theory, the natural parental medium is basically multi-component completely miscible carbonate-silicate melt with dissolved elemental carbon (in the frames of the peridotite-eclogite-boundary carbonatite-diamond system. The composition limits for diamond-forming melts are experimentally determined using the concentration barriers of diamond nucleation (CBDN) and correspond to the values (wt.%): $peridotite_{30}carbonatite_{70}$ and $eclogite_{35}carbonatite_{65}$ (Bobrov & Litvin, 2009). Generalized diagram of the parental medium composition is constructed (Litvin, 2010; Litvin et al., 2011). The diagram determines the boundaries for the phase region of parental media for diamond and inclusions. It has been ascertained in this case that compositions of the natural diamond-forming media belong to the carbonatite classification interval. In this work, study of physicochemical conditions of syngenesis of diamond and

mineral phases of peridotite and eclogite parageneses in carbonatite parental media is started at 8 GPa and 1200 – 1800°C.

Experimental study of formation of diamond and paragenetic phases This is evident from the phase region for parental media (fig.1) that their compositions are extremely changeable in respect tas content of silicate components ofp eridotite-pyroxenite and eclogite-grospydite parageneses so the indicators of the silicate/carbonate ratio. The value of mid-weighted composition for the parental medium is calculated for its concentration triangle «peridotite$_{30}$carbonatite$_{70}$ - eclogite$_{35}$carbonatite$_{65}$–boundary carbonatite» (composition 10 in the fig. 1 and in the table. 1). Experimental investigation of diamond and inclusions syngenesis is started within the section (wt. %) boundary carbonatite–
(peridotite$_{30}$carbonatite$_{70}$)$_{50}$(eclogite$_{35}$carbonatite$_{65}$)$_{50}$

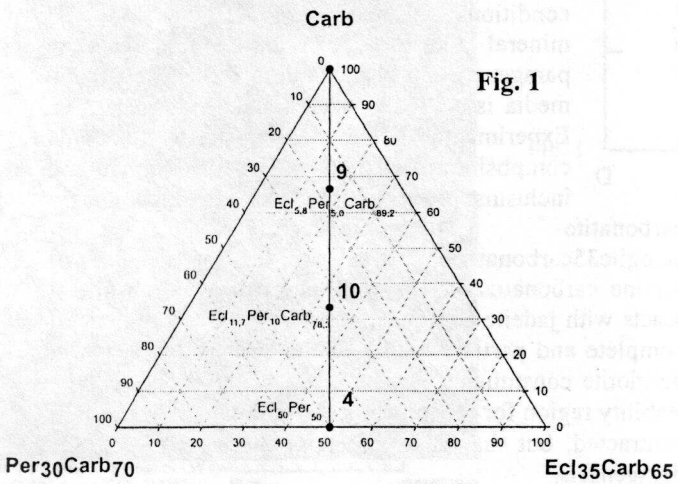

Fig. 1

which is formally the composition triangle for the parental media onto two parts – peridotitic and eclogitic. The starting experimental compositions №№ 9, 10 and 4 are given in the table 1 together with the boundary compositions used at their calculations.

Experimental studies were carried out in toroidal apparatus anvil-with-hole;the method details are characterized in the paper (Litvin et al., 2008). The results of microprobe analyses of the experimental phases including melts formed at temperature 1600 – 2000 °C, silicate minerals (garnet and clinopyroxene) and carbonate mineral (Mg-Fe-carbonate) at temperature 1400 – 1600°C , - are given in the table 2. Experimental data testify to that phases of the eclogite paragenesis are exclusively formed within the section boundary carbonatite – (peridotite$_{30}$carbonatite$_{70}$)$_{50}$(eclogite$_{35}$carbonatite$_{65}$)$_{50}$where as phases of the peridotite paragenesis are not presented. There is important to underline that such characteristic minerals of peridotite as olivine and orthopyroxene are absent. This is evidence of reaction interaction with the other components of the system under study. In other words, reaction "eclogitization" of peridotite is observed. Carbonatization reactions of peridotite Mg-minerals which were established in experiments at lower pressures (Wyllie, Huang, 1976), as well as reaction between olivine and jadeite components resulting in garnetization of olivine (Gasparik, Litvin, 1997) reveal themselves as important factors.

Table 1.Boundary compositions of the generalized diagram of parental media, the phase region of the parental media, and compositions of starting materials used in experiments at 8.0 GPa.

Composition	Oxides (wt. %)							
	K_2O	Na_2O	MgO	FeO	CaO	Al_2O_3	SiO_2	CO_2
Boundary Per		0.52	37.12	11.35	2.49	3.48	45.04	
Boundary Ecl		3.71	8.51	15.24	9.04	15.76	47.74	
Boundary Carb	18.55	1.69	8.30	15.89	15.08			40.49
CBDN Per$_{30}$Carb$_{70}$	12.99	1.34	16.95	14.53	11.31	1.04	13.50	28.34
CBDN Ecl$_{35}$Carb$_{65}$	12.08	2.40	8.38	15.65	12.95	5.52	16.70	26.30
№ 9	16.55	1.72	9.99	15.59	14.05	0.99	5.01	36.10
№10	13.30	1.80	12.80	14.80	12.40	1.90	14.43	28.00
№ 4	12.54	1.87	12.67	15.09	12.13	3.28	15.10	27.32

*Footnote to Table 1.*Symbols: Per - peridotite ,Ecl - eclogite, Carb - carbonatite; CBDN – concentration barrier of diamond nucleation; experimental compositions expressed through boundary constituents (wt. %): № 9 - Ecl$_{5.8}$Per$_{5.0}$Carb$_{89.2}$, №10 - Ecl$_{11.7}$Per$_{10.0}$Carb$_{78.3}$, № 4 - Ecl$_{17.5}$Per$_{15.0}$Carb$_{67.5}$.

Sampl	T,°C	Phases	Oxides(wt.%)							
			K_2O	Na_2O	MgO	FeO	CaO	Al_2O_3	SiO_2	CO_2
№9	1600	L	6.6-16.1	1.3-2.1	2.6-3.9	4.0-4.8	5.1-6.5	0.3-0.4	1.6-2.2	45.0-50.0
	1400	Carb	0.12	0.02	24.77	23.01	3.52		0.21	48.35
		Cpx	0.79	1.85	9.98	14.19	18.78	1.94	52.47	
		Grt		0.25	5.61	25.56	15.57	11.90	40.93	
№10	2000	L	4.8-8.5	0.7-1.4	2.3-3.9	3.5-4.0	3.1-4.1	1.0-3.0	4.0-6.0	30.0-50.0
	1400	Cpx	1.45	2.31	13.41	10.47	15.49	3.05	53.82	
		Grt		0.11	10.18	19.52	7.22	21.61	41.36	
№4	1800	L	5.0-5.5	0.7-3.5	1.7-5.8	10.6-13.9	6.5-10.9	1.5-3.7	12.4-18.9	40.5-53.0
	1600	Carb	0.65	0.18	17.89	23.86	7.01	0.09	0.49	49.83
		Cpx	0.56	2.50	9.88	14.91	15.76	2.87	53.52	Cpx
		Grt		0.26	5.85	24.16	12.95	17.98	38.80	Grt
	1400	Cpx	1.06	2.84	11.70	10.04	17.92	3.72	52.72	1400
		Grt		0.11	10.00	22.60	8.06	19.11	40.12	Grt

Table 2. Representative compositions of phases obtained in experiments at 8.0 GPa.

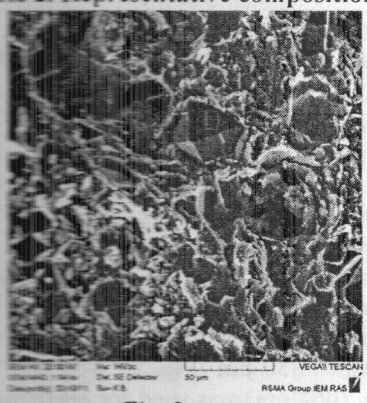

Fig. 2

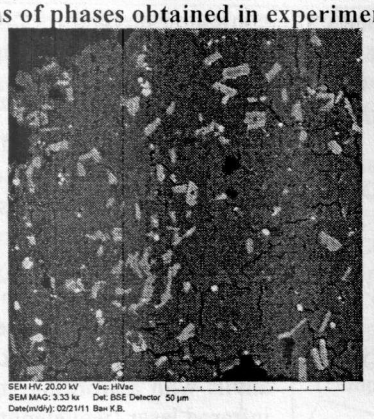

Fig. 3

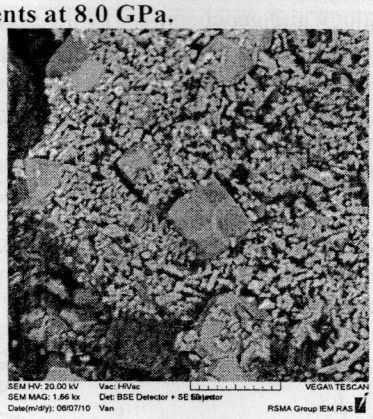

Fig. 4

Mass crystallization of diamond in melt oversaturated with dissolved elemental carbon in the sample № 10 of mid-weighted composition is demonstrated in the fig. 2 (sample № 2429, 2000°C). In the fig.3 (sample № 2450, composition № 9, 1400°C):eclogite assemblage Cpx + Grt with Mg-Fe-carbonate is shown, Ol andOpx are not determined. Fig. 4 (sampleNo 2270, a mode lsystem Fo-Di-Jd-Dol, 1200°C) demonstrates process of garnetization of olivine: the sample contains Grt and Cpx whereas forsterite (major component of olivine) is not detected.

Conclusion Experimental modeling of diamond and inclusions in parental medium which contains peridotite and eclogite minerals reveals physicochemical conditions of syngenetic crystallization of diamond and minerals of eclogite paragenesis (Cpx, Grt). Therewith, processes of carbonatization and garnetization of olivine and orthopyroxene suppress formation of characteristic minerals of peridotite paragenesis.

This study is supported by the grants of RFBR 11-05-0040 and SS-3564.2011.5.

References

1. Bobrov A.V., Litvin Yu.A. (2009), Peridotite-eclogite-carbonatitesystemsat7.0-8.5 GPa: concentrationbarrierofdiamondnucleationandsyngenesisofitssilicateandcarbonateinclusions, *Russian Geology and Geophysics*, *Vol. 50*, № 12, pp. 1571-1587.
2. Gasparik T., LitvinYu.A. (1997), Stability of $Na_2Mg_2Si_2O_7$ and melting relations on the forsterite-jadeite join at pressures up to 22 GPa,*European Journal of Mineralogy*, Vol. 9, pp. 311-326.
3. Litvin Yu.A. (2007), High-pressure mineralogy of diamond genesis, *Advances in High-Pressure Mineralogy (Ohtani E., ed.): Geological Society of America Special Paper 421*, pp. 83-103, doi: 10.1130/2007.2421(06).
4. Litvin Yu.A. (2009), The physicochemical conditions of diamond formation in the mantle matter: experimental studies *Russian Geology and Geophysics*, *Vol. 50*, № 12, pp. 1530-1546.
5. Litvin Yu.A. (2010), Physicochemical conditions of origin of natural diamond and heterogeneous substance of primary inclusions therein, Proceedings of *XI RMS General Meeting «Modern Mineralogy: from theory to practice», Saint Petersburg, 12-15 October 2010 г.*,pp. 77-78.
6. Litvin Yu.A., Litvin V.Yu., Kadik A.A. (2008), Peculiarity of diamond crystallization in melts of the mantle silicate-carbonate-carbon system by experiment data at7.0 – 8.5 GPa, *Geochemistry International*, №6.
7. Litvin Yu.A., Vasiliev P.G., Bobrov A.V., Okoemova V.Yu., Kuzyura A.V. (2011),Parental media of diamonds and primary inclusions by the data of physicochemicalexperiment, *Transactions of ESD RAS* (in this issue).
8. Wyllie P.J., Huang W.-L. (1976). Carbonation and melting reactions in the system CaO – MgO – SiO_2 – CO_2 at mantle pressures with geophysical and petrological applications, Contributions to Mineralogy and Petrology, Vol. 54, pp. 79-107.

Spivak A.V.[1], Dubrovinsky L.S.[2], Litvin Yu.A.[1] Congruent melting of Ca-carbonate in static experiment at 3500 K and 10-22 GPa

[1] IEM RAS; [2] Bayerisches Geoinstitut, Bayreuth

Key words: Super deep diamonds, transition zone, lower mantle, parental media, carbonate melts, phase diagram of CaCO3.

Carbonate melts have a crucial role for diamond forming carbonatite medium: (1) they are effective solvents of silicates, alu minum silicates, oxides; (2) carbonate melts are the basis of completely miscible carbonate-silicate and carbonate-silicate-oxide melts. Solid carbon (diamond and metastable graphite) is very soluble in the atomic form in these melts at the *PT* conditions of diamond stability [*Spivak et al.*, 2008]. Currently, information about the phase state of carbonates is contradictory for the conditions of the transition zone and lower mantle.

The melt of $CaCO_3$ undergoes decomposition by the reaction of $CaCO_3$ = CaO + CO_2 in the shock-wave experiments at 3200 - 3500 K and 80 GPa [*Ivanov AB, Deutsch A.*, 2002]. However, the direct evidence of decomposition reaction of carbonate melt at the maximum degree of compression or under the influence of high residual temperature after short-term relief to the normal pressure could not be obtained in the shock-wave experiment. Nevertheless, the available experimental data and the calculated equations of state of $CaCO_3$ and its decomposition products CaO and CO_2 summarized in a phase diagram of $CaCO_3$ (Fig. 1). Congruent melting curve of $CaCO_3$ was studied in a static experiment up to 7 GPa, and extrapolated on the basis of the equation of state [*Irving A.J., Wyllie P.J.*, 1973].

In the interval 10 - 30 GPa the congruent melting field $CaCO_3$ is limited by the melting curve of $CaCO_3$ at 2100 - 2500 K and the proposed curve of decomposition of $CaCO_3$ melt to CaO and CO_2 at high temperatures 3500 - 3800 K (Fig. 1).

Meanwhile, accurate understanding of physical and chemical behavior of $CaCO_3$ and other carbonates is of fundamental significance for a number of important

problems of mineralogy and geochemistry of the transition zone and lower mantle. Especially, genesis of super deep diamonds, as well as the origin and evolution of carbonate-containing melts (carbonatites, kimberlites, etc.) are among the problems.

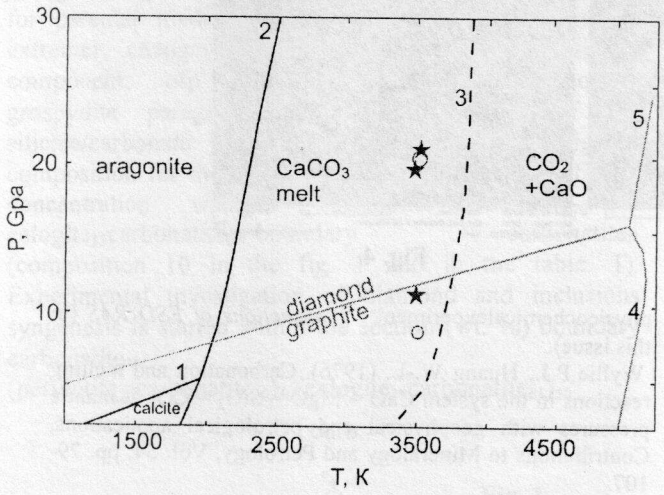

Fig. 1. Phase diagram of the Ca-carbonate [*Ivanov AB, Deutsch A.*, 2002] (thick lines), combined with the phase diagram of carbon [*Bundy FP et al.*, 1996] (thin lines). Legend: 1 - boundary of polymorphic transformation of calcite-aragonite, 2 - congruent melting curve of calcite and aragonite, 3 - decomposition curve of Ca-carbonate melt to CaO and CO_2, 4 - the melting curve of graphite, 5 - the melting curve of diamond. Stars - the experimental points of the authors, circles - experimental points by [*Bayarjargal L. et al.*, 2010].

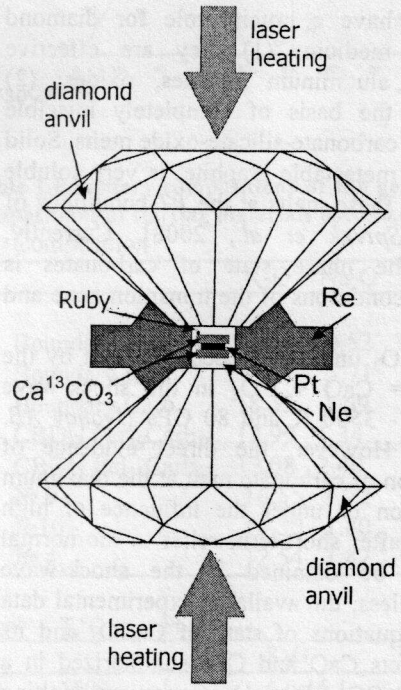

Fig. 2. The diamond anvil cell

The goal of this work is experimental study of the phase state of $CaCO_3$ at static pressure of 11 - 22 GPa (generated in the apparatus with diamond anvils) and temperatures up to 3500 K, obtained by laser heating of a strongly compressed sample (for details see [*Eremets M.*, 1996]). The *PT*-parameters of the experiment is consistent with the physical conditions of formation of super deep diamonds, which overlap with the possible field of congruent melting of Ca-carbonate (Fig. 1). An important feature of this work is the use of isotope individual carbonate $Ca^{13}CO_3$ that excludes the possibility of distortion of results of ^{12}C of the anvils (natural diamond) is unexpectedly involved into products of the experiments.

Starting materials were chemical reagents of $Ca^{13}CO_3$ (prepared on the basis of the isotope ^{13}C). The experimental sample consists of two layers of powder $Ca^{13}CO_3$, and a thin layer of platinum powder between them. The sample is placed into the hole of 150 μm diameter (filled by an inert gas neon) in a metallic gasquet of rhenium. The gasquet is clamped between the diamond anvils with a working surface 350 μm (Fig. 2). Nd: YLF infrared laser (wavelength 1064 nm) was used for heating. The duration of heat was about 5 minutes.

The pressure in the sample is determined by the shift of the ruby luminescence. A ruby grain of ~ 5 μm size is placed inside the sample. During lowering the heating temperature to the room value, the sample has remained under strong compression inside Re gasquet. Products of experiments were studied using micro-Raman spectroscopy. The system LabRam with He-Nd-laser (exciting wavelength 632 nm) was used for register Raman spectra. Spectra from different parts of the sample collected at the gradual decompression, as well as after quenching, when the sample is completely extracted from the working holes in rhenium gasquet.

Experimental samples are marked (Fig. 3) with the visible zone of calcium carbonate melting (about 50 microns) in experiments at 20-22 GPa and 3500 K (Fig. 1). The sample in the experiment at 11 GPa and 3500 K are not visualy different from them, but their Raman spectra include a peak of graphite. The samples were not heated along the perimeter, and these areas were used for comparative estimation. Raman spectra of samples under pressure were collected before and after heating. Also, the spectra of $Ca^{12}CO_3$ and $C^{13}CO_3$, graphite on the basis of the isotopes ^{12}C and ^{13}C were obtained for the comparison.

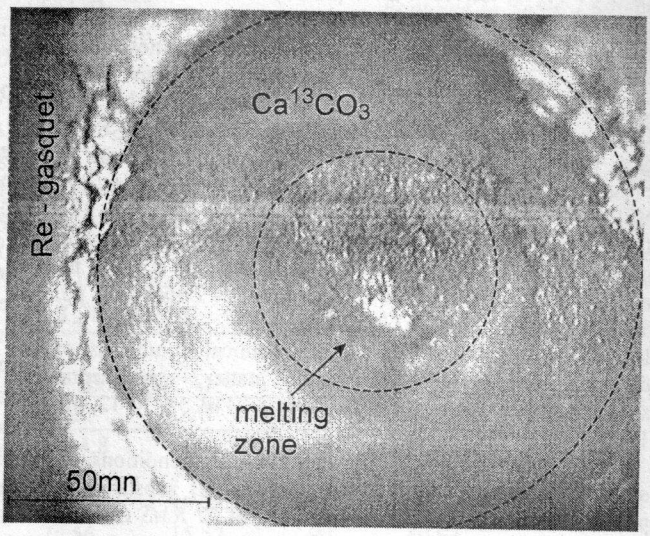

Fig. 3. Image of $Ca^{13}CO_3$ sample after melting and quenching under pressure

Representative Raman spectra of various matters are shown in fig. 4. Under normal conditions, Raman spectra $Ca^{12}CO_3$ have characteristic bands at 155, 280, 712 and 1086 cm^{-1} [*Rutt H.N., Nicola J.H.*, 1974]. The spectra of $Ca^{13}CO_3$ contain the main band at 153, 278, 710, 1086 cm^{-1}, and the spectra of graphite on the basis of the isotope ^{13}C

- the band at 1278 and 1535 cm^{-1}. Calcite on the basis of the isotope ^{13}C transforms into aragonite in experiments at high pressures and temperatures, as evidenced the spectra

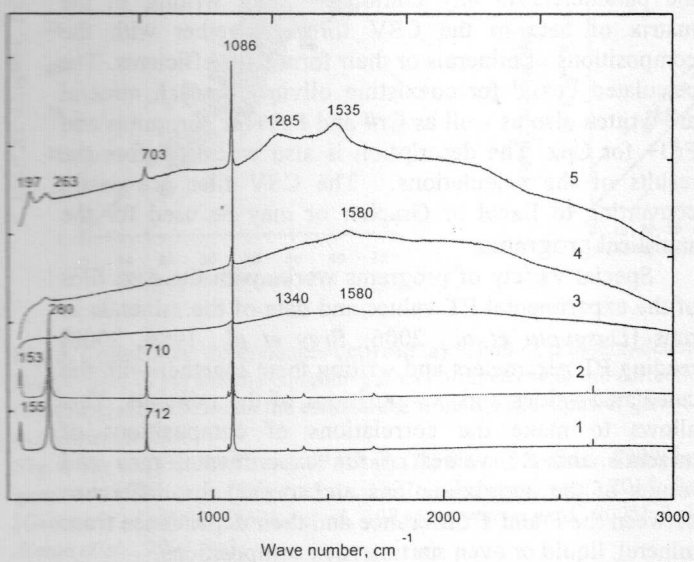

Fig. 4. Raman spectra of the experimental samples:
1 - $CaCO_3$ under normal conditions,
2 - $Ca^{13}CO_3$ under normal conditions,
3 - $Ca^{13}CO_3$ at 11 GPa and 3500 K (after extraction of the sample),
4 - $Ca^{13}CO_3$ at 20 GPa and 3500K (after extraction of the sample),
5 - $Ca^{13}CO_3$ at 21GPa and 3500 K (after extraction of the sample).

which have the characteristic bands of aragonite 703 and 197 cm^{-1} (according to their displacement due to the presence of the isotope ^{13}C). The most intense band at 1086 cm-1 is characteristic for the two polymorphic modifications of calcium carbonate and can not be used as a distinctive feature of them.

Graphite on the basis of the isotope ^{12}C was found in the central parts with a diameter of 50 microns after heating to 3000 K at 20-22 GPa. Raman spectra of the experimental samples contain bands of graphite ^{12}C, including a broad band with a peak in the range at 1580-1585 cm^{-1}, known as "band G", and a broad band with a peak in the range at 1340-1355 cm^{-1} - "band D". The position and width of the G band are determined by the perfection of graphite structure and the position of the D band is identified with various types of violations of the order in the structure of graphite. Because $Ca^{13}CO_3$ was used as the starting material, the formation of graphite ^{12}C by carbon ^{13}C from this carbonate should be entirely avoided entirely. Source of carbon for graphite ^{12}C could be just the carbon from diamond anvils. It can not exclude that in the experiments described in [*Bayarjargal L. et al.*, 2010], the same occurred. Thus, the effect of the congruent melting of $Ca^{13}CO_3$ is determined in experiments at 3000 - 3500 K and 20 GPa. However, the Raman spectra of the sample obtained at 11 GPa and 3500 K, contain a broad band G with a maximum in the range at 1528-1537 cm^{-1}, "echo" of the band at 1580 cm^{-1} and D band with a peak in the range at 1275-1285 cm^{-1}. In this case we can meet the formation of graphite phase, with a source of carbon from the calcium carbonate on the basis of ^{13}C isotope. The reality of this process is supported by *RT*-conditions of the experiment, which refers to the corresponding field on the carbon phase diagram (Fig. 1). This fact may testify of the reality of $Ca^{13}CO_3$ decomposition process on a two-step mechanism, which was discussed in [*Bayarjargal L. et al.*, 2010]. Characteristic bands of graphite were not observed in Raman spectra of "unheated" parts of the sample.

As a result of the experiments, it is showed that calcium carbonate m elts congruently at 20-21 GPa and 3500 K. The experimental data are in aggrement with the preliminary phase diagram of $CaCO_3$ [*Ivanov AB, Deutsch A.*, 2002], constructed on the basis of shock experiments and thermodynamic calculations. The data confirm the fact of congruent melting of $CaCO_3$ (aragonite) at 20 - 21 GPa and 3500 K. This means that the field of congruent melting of calcium carbonate is quite wide, extending from 2300 to 3500 - 3800 K at 20-21 GPa. However, the results o f experiments a t 11 GPa and 3500 K demonstrate the possibility of high-temperature phase boundary of the decomposition of $CaCO_3$ to CaO melt and compressed CO_2 fluid phase.

$CaCO_3$ is a representative inclusion in diamonds from transition zone and lower mantle. Existence of a broad field of $CaCO_3$ congruent melting allows us to consider deep carbonate melts based on $CaCO_3$ as a possible parental media for super deep diamonds.

Support: МК-913.2011.5, Program RAS №02, 10-05-00654, 11-05-00401, НШ-3654-2011-5.

References

1. Bayarjargal L., T.G. Shumilova, A. Friedrich, B. Winkler (2010), Diamond formation from $CaCO_3$ at high pressure and temperature, *Eur. J. Miner., V. 22,* P. 29-34.
2. Bundy F.P., W.A. Basset, M.S. Weathers, R.J. Hemley, H.K. Mao, A.F. Goncharov (1996), The pressure-temperature phase and transformation diagram for carbon; updated through 1994. *Carbon, V. 34,* № 2, P. 141-153.
3. Eremets M. (1996), *High Pressure Experimental Methods. New York, Oxford University Press Inc*, 390 p.
4. Irving A.J., P.J. Wyllie (1973), Melting relationships in CaO-CO_2 and MgO-CO_2 to 33 kbar, *Earth Planet. Sci. Lett., V. 20,* P. 220-225.
5. Ivanov A.B., A. Deutsch (2002), The phase diagram of CaCO3 in relation to shock compression and decomposition. *Phys. Earth Planet. Inter., V. 129,* P. 131-143.
6. Rutt H.N., J.H. Nicola (1974), Raman spectra of carbonates of calcite structure. *J. Phys. C: Solid State Phys., 7,* 4522-4528.
7. Spivak A.V., Yu.A. Litvin, A.V. Shushkanova, V.Yu. Litvin, A.A. Shiryaev (2008), Diamond formation in carbonate-silicate-sulfide-carbon melts: Raman- and IR-spectroscopy. *Eur. J. Mineral., 20,* 341-347

Ashchepkov I.V. Program of the mantle thermometers and barometers: usage for reconstructions and calibration of PT methods.

Institute of Geology and mineralogy SB RAS, Novosibirsk

Key words: Mantle, thermobarometry, layering, lithosphere, PT program

Program description Original monomineral thermobarometers for mantle peridotites for clinopyroxene, garnet, chromite and ilmenites for the mantle peridotites were statistically calibrated on the PT estimates for mantle peridotites [*Ashchepkov et al.*, 2010] were tested using the mineral phases obtained in high pressure experiments with the natural peridotites (380

runs) [7-9 etc] and eclogites (240 runs)[10 etc]. They are in a good In the original program of that written on FORTRAN are assembled the most reliable methods of mineral thermometers (45) and barometers (36) and oxybarometers (5), including original monomineral and methods [*Ashchepkov,* 2003 *Ashchepkov et al.*, 2008; 2009; 2010; 2011] for the mantle peridotites bases on the compositions of on clinopyroxene, garnet, chromite and ilmenite. Program reads the text files, which converted from Excel. Original data include standard silicate compositions for 12 components. The text file includes 15 columns of 8 symbols. The first is file name which is the same for all the minerals in the association. The second is indicator symbol for phases. E- enstatite, D - diopside, O- olivine, S-spinel, G- garnet, I –ilmenite, A- amphibole, F – phlogopite, P-plagioclase, L- liquid, R- bulk rock. The last column may contain description of the mineral or association up to 64 symbols. Monomineral methods use calculated values for Fe#Ol or Fe#Cpx. The input from console includes file name (8 symbols) (A8), then amount of PT pairs of numbers thermometers and barometers (2I2) and one for FO2 method. Program allows input of the iteration numbers (to 25). It allow to choose whether to use the calculated Fe3+ for the minerals and also.

The program is reading mineral compositions detecting them by mineral indexes till name of the association are the same and start the estimations of PT values when read different names. They are going to the dispatcher points sending to the thermometers and barometers according to the input numbers. It is performing calculation for each pair till the difference of the temperatures is higher 1° or less then iteration number made then goes to next pair. The values of calculates pairs are writing in the matrix. It is writing in new line when the new association starts.

The results of the calculations of pairs (to 15) PT of the parameters in any combination are writing in the matrix of data in the CSV format together with the compositions of minerals or their formula coefficients. The calculated Fe#Ol for coexisting olivine for each mineral are written also as well as Cr# and Fe3+for chromites and Fe3+ for Cpx. The description is also writing before the results of the calculations. The CSV files are easily converting to Excel or Grapher or may be used for the statistical programs.

Special variety of programs works with the data files of the experimental PT values and data of the minerals in runs [*Dasgupta et al.*, 2006; *Brey et al.,* 1990, 2008] reading PT parameters and writing them together with the calculated values and compositions of the minerals. This allows to make the correlations of compositions of minerals and PT values of the experimental runs and results of the approximations and to find the difference between the P and T difference and their dependence from mineral, liquid or even starting rock compositions.

Applications Recently new version of the peridotite-pyroxenites Cpx barometer [*Ashchepkov et al.*, 2003-2011] was obtained using about 300 experimental runs for basalts and peridotites and pyroxenites. This universal barometer [*Ashchepkov et al.*, 2011] reveals rather good calibration and agreement with the most reliable methods of mantle thermobarometry [*Brey and Kohler, 1990*; *Krogh,* 1988; *Nimis and Taylor,* 2000; *McGregor*, 1974; *O'Neill and Wood,* 1979; *Taylor et al.*, 1998; *O'Neill and Wall*, 1987] (Fig.1-3,5).

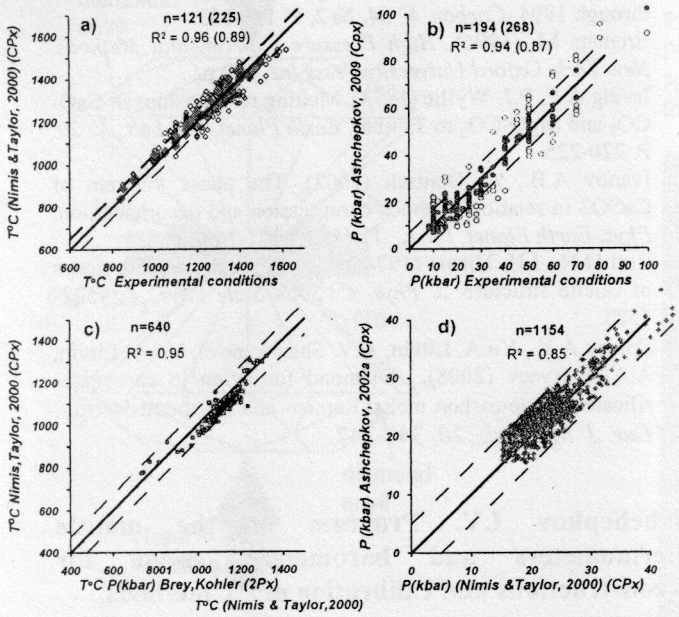

Fig. 1. Correlation of the determinations of the from the universal equation of clinopyroxene barometer [*Ashchepkov,* 2011] according to the experimental data (b) in the peridotite system and the comparison of estimations according to this equation and Cr-Tchermakite barometer [*Nimis and Taylor,* 2000].

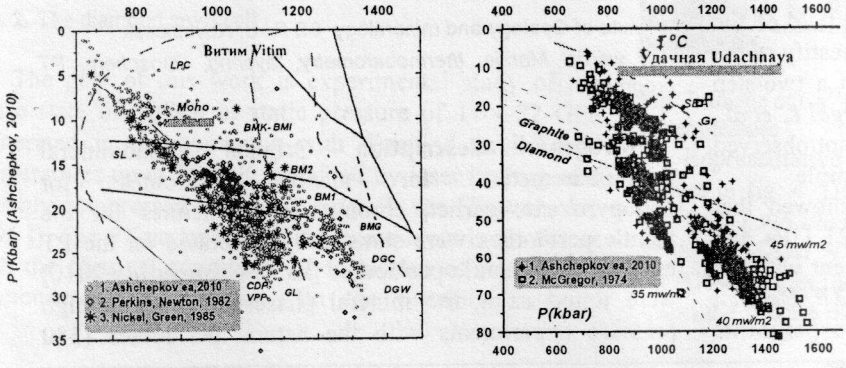

Fig. 2. Estimations of (temperature and) of pressure with the universal version of clinopyroxene barometer [*Ashchepkov,* 2011] in the comparison with the estimations according to orthopyroxene methods (see legend) for the xenoliths from basalts from the Vitim plateau (a) and for the xenoliths from Udachnaya pipe[*Boyd et al.*, 1997; *Ionov et al.*, 2010].

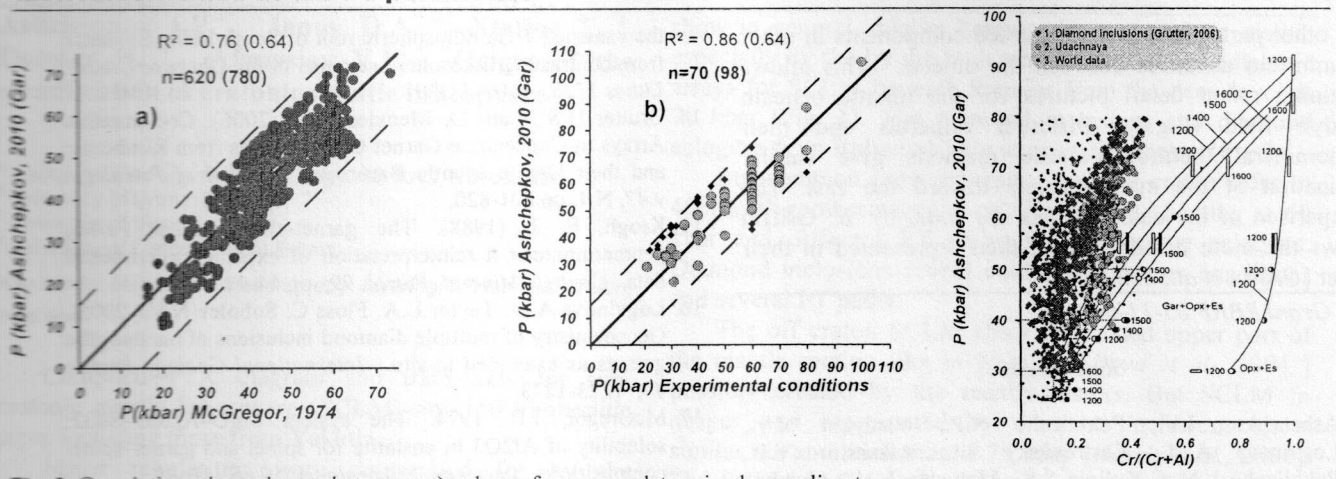

Fig. 3. Correlations dependences between: **a)** values of pressure, determined according to [*McGregor*, 1974] and the equation garnet barometer with the corrections.
(b). Correlations between the estimations from the equations of garnet barometer and experimental data.

Fig. 4 The diagram Cr/Cr+Al - P (kbar) [*Turkin and Sobolev*, 2009] according to experimental data and values calculated for natural garnets 1- Udachnaya [Boyd, et al ., 1997; *Ashchepkov et al.*, 2010; *Pokhilenko et al.*, 1999; Sobolev , 1977]; 2. Diamond associations [*Grutter et al.*, 2006; *Sobolev et al.*, 1984; *Logvinova et al.*, 2005]; 3. Worldwide kimberlites [*Sobolev,* 1977; *Burgess and Harte*, 2004; *Simon et al* ., 2007 etc].

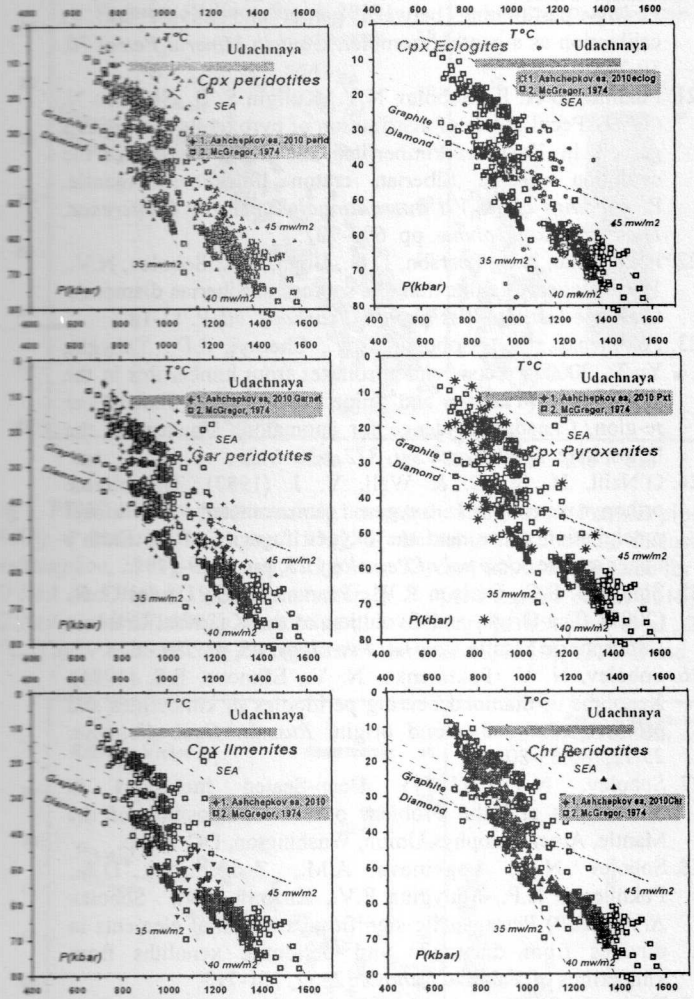

Fig. 5. PT estimates using the modified methods *[Ashchepkov et al.,* 2010; 2011, *Krogh,* 1988; *Nimis and Taylor,* 2000, *McGregor,* 1974; *O'Neill ant Wood,* 1979, *Taylor et al.,* 1998; *O'Neill and Wall,* 1987] for the pressure estimates in comparison with the Opx - based method *[Brey and Kohler, 1990-McGregor,* 1974**].**

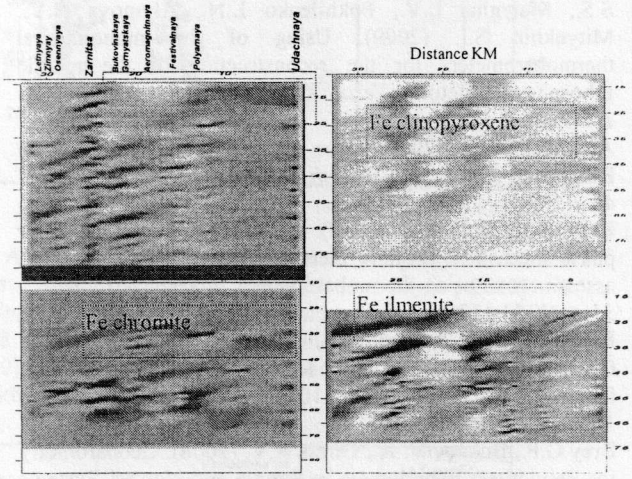

Fig.6. The cross -sections of the Daldyn field in Yakutia. From Zarnitsa to Udachnaya pipe, data from [*Ashchepkov et al.*, 2010]

The new improvements of the garnet barometer [Ashchepkov et al., 2008; 2010] give much better coincidence for the experimental systems [Brey, G.P. and Kohler, 1990; Brey et al., 2009] and garnet bearing peridotitic mantle xenoliths as well as garnets from diamond inclusions [Logvinova et al., 2005; Sobolev et al., 1984] and from diamond associations [Grutter et al., 2006; Sobolev et al., 1984] (Fig.3). Comparison with the diagram based on the experimental data show that most of the pressures in the natural associations are overestimating the experimental values for the same Cr/(Cr+Al) values (Fig.4) [Turkin and Sobolev, 2009].

A newly modified version of the programs includes the methods for the T and P estimates according to the precise data for olivine [*Sobolev et al.,* 2009*; De Hoog,* 2010]. They single grain temperatures for olivine show a good correlation with the pyroxene estimates (*Ashchepkov et al.,* 2010).

For the works with Grapher software the calculated values of pressures are writing together with the Fe# or

any other parameters including trace components in other column and distances between the objects. This allows obtaining rather detail pictures for the mantle beneath Daldyn field (Fig.6). Different minerals and their monomineral thermobarometric methods give similar inclination of the mantle layers toward the east. The comparison of the data obtained for India by W. Griffin shows the more detail layering then represented in their paper [*Griffin et al.*, 2009].

Grant RBRF 05-11-00060a

References

1. Ashchepkov I.V., Pokhilenko N.P., Vladykin N.V., Logvinova A.M., Kostrovitsky S.I., Afanasiev V.P., Pokhilenko L.N., , Kuligin S.S., Malygina L.V., Alymova N.V., Khmelnikova O.S., Palessky S.V., Nikolaeva I.V., Karpenko M.A., Stagnitsky Y.B. (2010). Structure and evolution of the lithospheric mantle beneath Siberian craton, thermobarometric study. *Tectonophysics, 485*, pp.17-41.
2. Ashchepkov I. V., Pokhilenko N. P., Vladykin N.V., Rotman A.Y., Afanasiev V.P., Logvinova A.M., Kostrovitsky S.I., Pokhilenko L.N., Karpenko M.A., Kuligin S.S., Malygina E.V., Stegnitsky Y.B., Alymova N.A., Khmelnikova O.S. (2008). Reconstruction of mantle sections beneath Yakutian kimberlite pipes using monomineral thermobarometry. *Geological Society, London, Special Publications, .293.* pp. 335 – 352.
3. Ashchepkov I.V., André L., Downes H., Belyatsky B.A. (2011). Pyroxenites and megacrysts from Vitim picrite-basalts (Russia): polybaric fractionation of rising melts in the mantle? *Journal Asian Earth Sciences* (in press).
4. Ashchepkov I.V., Vladykin N.V., Logvinova A.M., Kuligin S.S., Malygina L.V., Pokhilenko L.N., Alymova N.V., Mityukhin S.I. (2009). Using of the monomineral thermobarometers for the reconstruction of the mantle lithosphere structure. *Vestn. Otd.nauk o Zemle RAN. № 1(27).*
5. Ashchepkov I.V. (2003). More precise equation of the Jd-Di Barometer. *Herald of the Earth department RAS.* № 1. P. 45-46.
6. Brey, G.P., Kohler, T. (1990). Geothermobarometry in four phase lherzolites II: new thermo-barometers and practical assessment of using thermobarometers. *Journal of Petrology 31*, pp.1353-1378.
7. Brey G.P., Kohler T., Nickel K.G. (1990). Geothermobarometry in four-phase lherzolites I. Experimental results from 10 to 60 kbar. *Journal of Petrology 31*, 1313-1352.
8. Brey G.P., Bulatov V. K., Girnis A.V. (2008). Geobarometry for Peridotites: Experiments in Simple and Natural Systems from 6 to 10 GPa. *Journal of Petrology, v.41/1* pp.3-24
9. Boyd, F.R., Pokhilenko, N.P., Pearson, D.G., Mertzman, S.A., Sobolev, N.V., Finger, L.W., 1997. Composition of the Siberian cratonic mantle: evidence from Udachnaya peridotite xenoliths. *Contrib. Mineral. Petrol. 128*, 228-246.
10. Burgess S.R., Harte B. (2004). Tracing lithosphere evolution through the analysis of heterogeneous G9-G10 garnets in peridotite xenoliths, II: REE chemistry. *Journal of Petrology 45*. Iss. 3. pp. 609-634
11. Dasgupta R., Hirschmann M.M., Stalker K. (2006) Immiscible Transition from Carbonate-rich to Silicate-rich Melts in the 3 GPa Melting Interval of Eclogite + CO2 and Genesis of Silica-undersaturated Ocean Island Lavas *Journal of Petrology, 47*, pp. 647 - 671.
12. De Hoog J.C., Gall L., Cornell, D.H. (2010). Trace-element geochemistry of mantle olivine and application to mantle petrogenesis and geothermobarometry. *Chemical Geology, 70*, 196-215
13. Griffin W.L., Kobussen A.F., Babu E.V.S.S.K., O'Reilly S.Y, Norris R., Sengupta P. (2009)A translithospheric suture in the vanished 1-Ga lithospheric root of South India: Evidence from contrasting lithosphere sections in the Dharwar Craton. *Lithos 112S*, 1109–1119.
14. Grutter H.S., Latti D. Menzies A.H. (2006). Cr-Saturation Arrays in Concentrate Garnet Compositions from Kimberlite and their Use in Mantle Barometry. *Journal of Petrology, v.47*, N 4, pp.801-820.
15. Krogh, E. J. (1988). The garnet-clinopyroxene Fe-Mg geothermometer a reinterpretation of existing experimental data. *Contrib. Mineral. Petrol. 99*, pp.44-48
16. Logvinova A.M. Taylor L.A. Floss C. Sobolev N.V.(2005). Geochemistry of multiple diamond inclusions of harzburgitic garnets as examined in-situ. *International Geology Review 47*, 1223-1233
17. McGregor, I.D. 1974. The system MgO–Al2O3–SiO2: solubility of Al2O3 in enstatite for spinel and garnet–spinel compositions. *American. Mineralogist 59* pp.110–19.
18. Nimis P., Taylor W. 2000. Single clinopyroxene thermobarometry for garnet peridotites. Part I. Calibration and testing of a Cr-in-Cpx barometer and an enstatite-in-Cpx thermometer. *Contrib. Mineral. Petrol. 139*, pp.541-554.
19. Nickel K.G., Green D.H. (1985) Empirical thermobarometry for garnet peridotites and nature of lithosphere, kimberlites and diamonds. *Earth. Planet. Sci. Lett. v.73*, p.153-170.
20. O'Neill H.St.C, Wood B.J. (1979). An experimental study of Fe-Mg- partitioning between garnet and olivine and its calibration as a geothermometer. *Contrib Mineral Petrol 70*, 59-70
21. Pokhilenko N. P., Sobolev N.V., Kuligin S. S., Shimizu N. (1999). Peculiarities of distribution of pyroxenite paragenesis garnets in Yakutian kimberlites and some aspects of the evolution of the Siberian craton lithospheric mantle. *Proceedings of the VII International Kimberlite Conference. The P.H. Nixon volume.* pp. 690-707.
22. Pokhilenko, N.P., Pearson, D.G., Boyd, F.R., Sobolev, N.V., 1991. Megacrystalline dunites: sources of Siberian diamonds. *Carnegie Institute Washington. Yearbook. 90*, P. 11-18.
23. Pokhilenko, N.P., Sobolev, N.V., Chernyi, S.D., Yanygin, Yu.T., 2000. Pyropes and chromites from kimberlites in the Nakyn field (Yakutia) and Snipe Lake district (Slave River re-gion, Canada): evidence for anomalous structure of the lithosphere. *Dokl. Earth Sci. 372*, 638–642.
24. O'Neill, H. St. C. & Wall, V. J. (1987). The olivine orthopyroxene-spinel oxygen geobarometer, the nickel precipitation curve, and the oxygen fugacity of the Earth's upper mantle. *Journal of Petrology 28*, pp. 1169-1191.
25. Simon N. S.C., Carlson R.W., Pearson D. G., Davies G. R. (2007). The Origin and Evolution of the Kaapvaal Cratonic Lithospheric Mantle. *Journal Petrology;.48*, pp.589 - 625.
26. Sobolev, N. V., Pokhilenko, N. V., Efimova, E.S. (1984). Xenoliths of diamond bearing peridotites in kimberlites and problem of the diamond origin. *Russian Geol. Geophys. 25/12*, pp.63-80.
27. Sobolev, N.V., (1977). Deep-Seated Inclusions in Kimberlites and the Problem of the Composition of the Mantle. Amer. Geophys.Union, Washington, DC. 279 p.
28. Sobolev N.V., Logvinova A.M., Zedgenizova D.A., Pokhilenko N.P., Malygina E.V., Kuzmin D.V., Sobolev A.V. (2009) Petrogenetic significance of minor elements in olivines from diamonds and peridotite xenoliths from kimberlites of Yakutia. *Lithos 112, S2*, 701-713.
29. Taylor W.R., Kammerman M., Hamilton R. (1998). New thermometer and oxygen fugacity sensor calibrations for ilmenite and chromium spinel-bearing peridotitic assemblages. *7th International Kimberlite Conference. Extended abstracts. Cape town.* 891-901
30. Turkin A.I., Sobolev N.V. (2009). Pyrope–knorringite garnets: overview of experimental data and natural parageneses. *Russian Geology and Geophysics, 50*, 1169-1182

Ashchepkov I.V.[1], Ionov D.A. [2], Ntaflos T. [3], Downes H. [4], Afanasiev V.P[1] Origin of the stratification of cratonic mantle lithosphere.

[1] Institute of Geology and mineralogy SB RAS, Novosibirsk;
[2] University of Lyone, France;
[3] University of Vienna, Austria;
[4] University of London, Great Britain

Key words: Mantle, thermobarometry, layering, lithosphere, craton, heat flow

Compiled PTX diagram and trans-sects for sub-cratonic mantle lithosphere (SCLM) >of 150 kimberlitic pipes including those from Yakutia.

Major regularities were determined for by the comparison of the PTX diagram for the subcratonic lithospheric mantle (SCLM) according to mantle xenoliths from large amount of the kimberlite pipes from N America Yakutia, Baltica , South and Central Africa. Proterozoic pipes from Africa like Premier Roberts Victor show in general higher heating degree which is visible especially by the by the high temperature PT subadiabatic arrays for SCLM beneath Premier from the deep level at 70 kbar (Fig. 1). The diamond inclusions and diamond eclogites from Roberts Victor support this thesis. (Fig 2).

But common pipes beneath Kaapvaal craton refer to 40mw/m^2 geotherm in the middle part and heating at 60 kbar and different PT paths for the mantle eclogites. Diamond inclusions reveal colder and deeper conditions and several PT paths.

The off craton SCLM show the heated upper part of the mantle section like in Namibia [*Boyd et al.*, 2004] possibly created by the mantle diapirs. But SCLM in deeper part represented by diamond inclusions show similar hot and thick mantle 75 кбар [*Harris et al.*, 2004]. The SCLM in Congo Kasai craton in Angola and Gunea show thicker and colder SCLM. But the rifted aria within craton show rather heated conditions like in Tansania, Labait volcano [*Aulbach et al.*, 2008] (Fig.5).

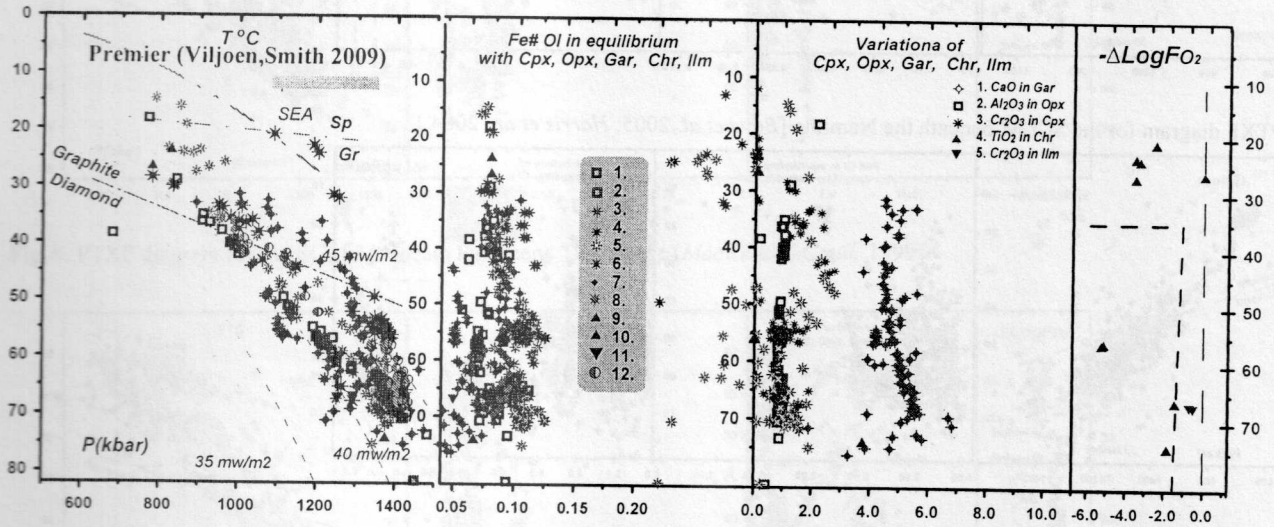

Fig 1. PTXF diagram for the mantle beneath the Proterozoic Premier pipe S Africa. Signs for orthopyroxene: 1. T°C [*Brey and Kohler*, 1990]) -P (kbar) [*McGregor*, 1974]. 2. the same for diamond inclusions; clinopyroxene: 3. T°C [*Nimis and Taylor*, 2000] – P [*Ashchepkov*, 2010]; 4. P and T°C *Nimis, Taylor* , 2000. 5. the same for eclogites; 6. the same fore diamond eclogites. Garnet: 7. T°C [*O'Neil and Wood*, 1979, monomineral]- P [*Ashchepkov et al.*, 2010]. 8. the same for the diamond inclusions; chromite: 9.T°C [*O'Neil and Wall*, 1987], monomineral]- P [kbar] [*Ashchepkov et al.*, 2010]; 10. the same for the diamond inclusions; 11. ilmenite: T°C [*Taylor et al.*, 1998]- P[kbar][*Ashchepkov et al.*, 2010]; 13. T°C and P [kbar] [*Brey and Kohler*, 1990]

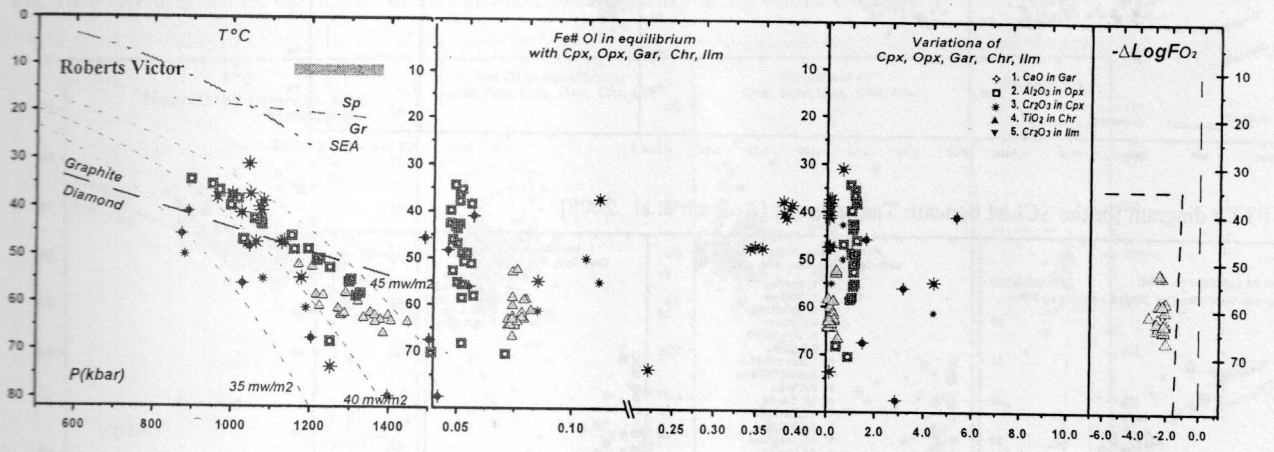

Fig 2. PTXF diagram for the SCLM beneath the Proterozoic Roberts Victor pipe S Africa. [*Hatton et al.*, 1979; *Jacob et al.*, 2005]

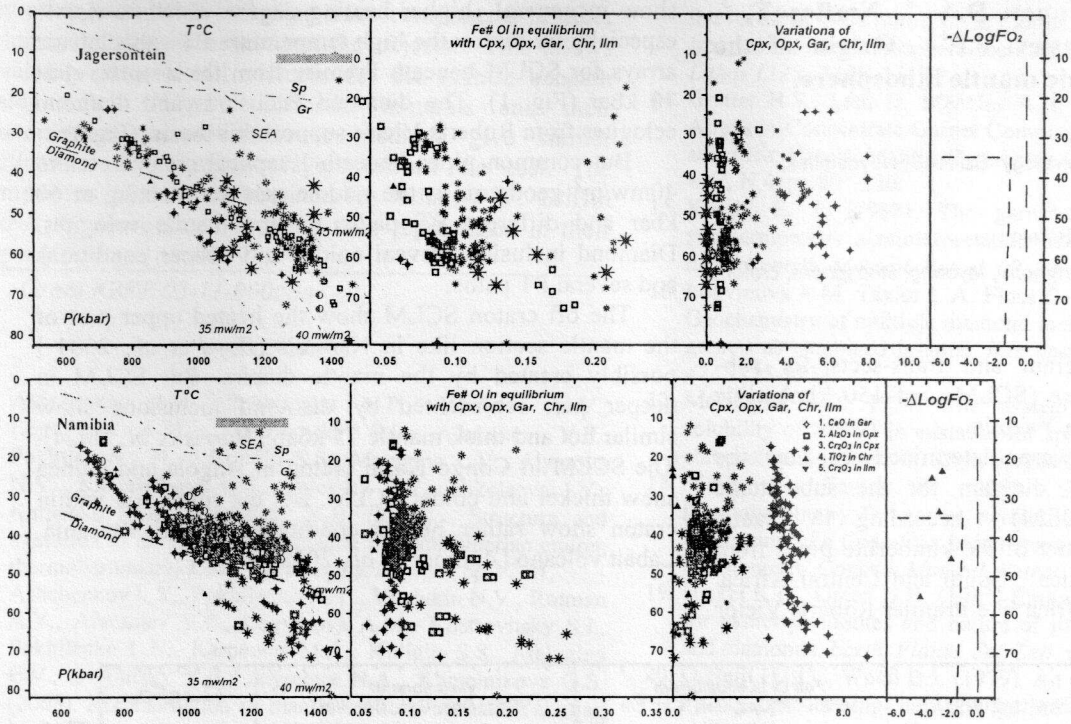

Fig 3. PTXF diagram for the SCLM beneath the Mesozoic Jagersfontein pipe S Africa [*Tappert et al.*,2005; *Tsai et al.*, 1979; *Winterburn et al.*, 1990]

Fig 4. PTXF diagram for the SCLM beneath the Namibia [*Boyd et al.*,2005; *Harris et al.*, 2004.]

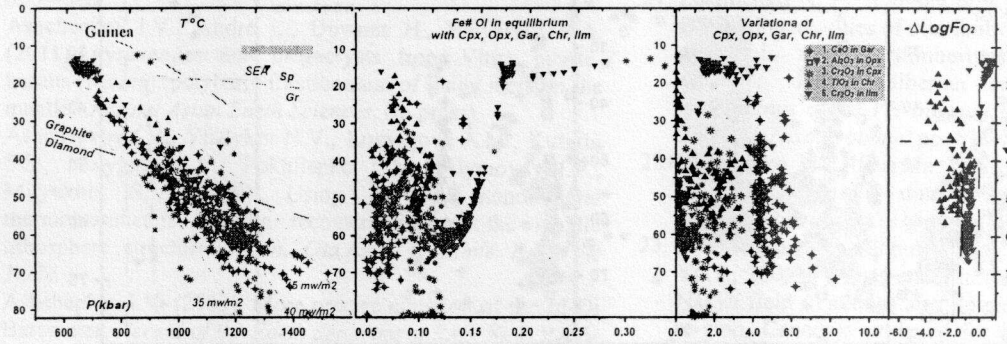

Fig 5. PTXF diagram for the SCLM beneath Guinea. Our data.

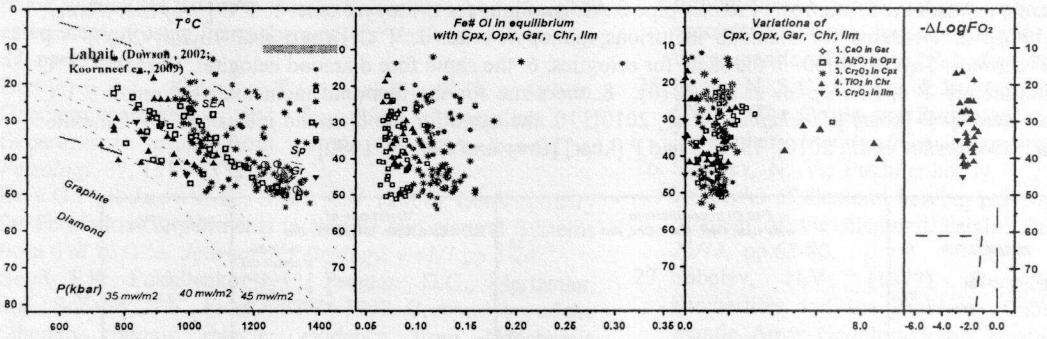

Fig. 6. PTXF diagram for the SCLM beneath Tansania rift [Aulbach et al., 2008].

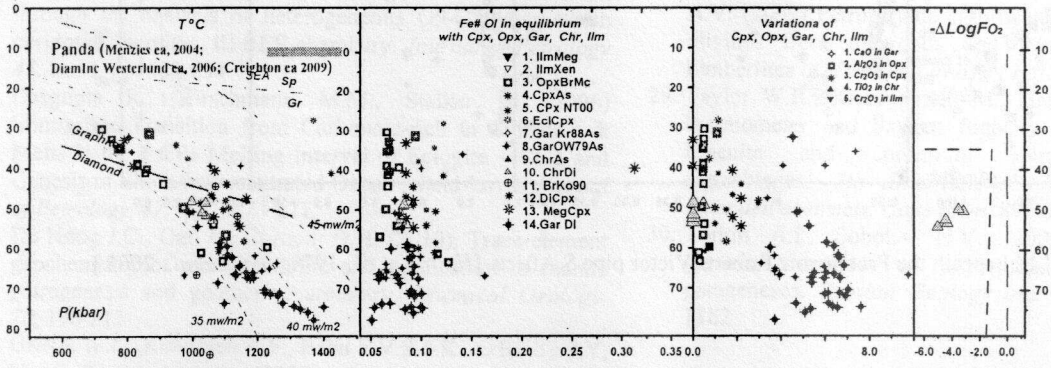

Fig. 7. PTXF diagram for the SCLM beneath Slave Craton [*Cartigny et al.*, 2009]

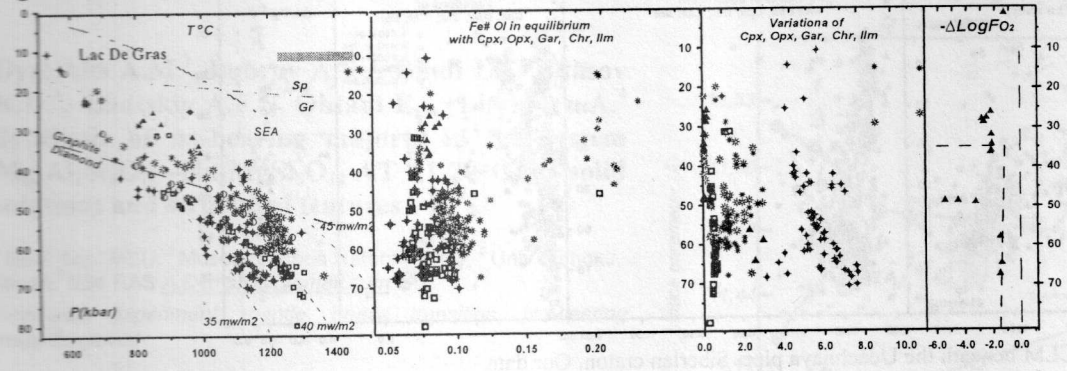

Fig. 8. PTXF diagram for the SCLM beneath Slave Craton [*Davies et al.*, 2004]

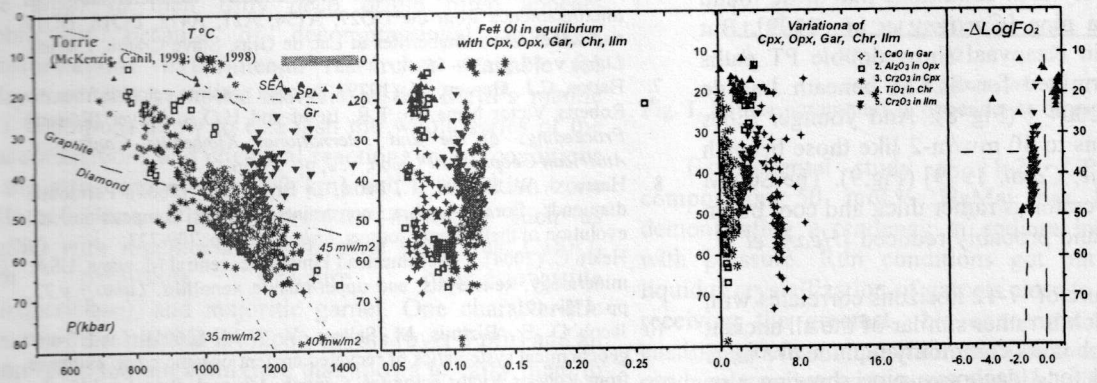

Fig. 9. PTXF diagram for the SCLM beneath Paleocene Torrie pipe [*MacKenzie, Canil*, 1999]

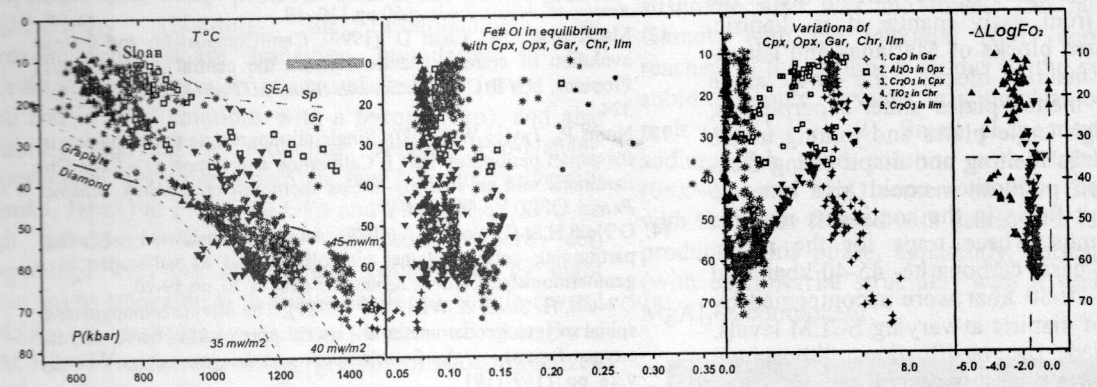

Fig. 10. PTXF diagram for the SCLM of the Paleozoic Sloan pipe Wyoming craton. Our data.

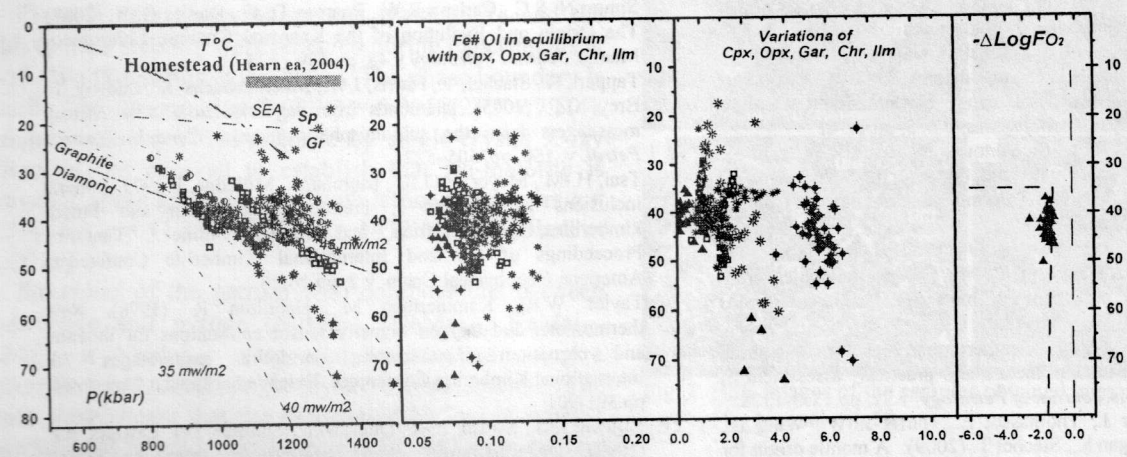

Fig.11. PTXF diagram for SCLM beneath Cretaceous Homestead pipe Wyoming craton. [*Hearn et al.*, 2004].

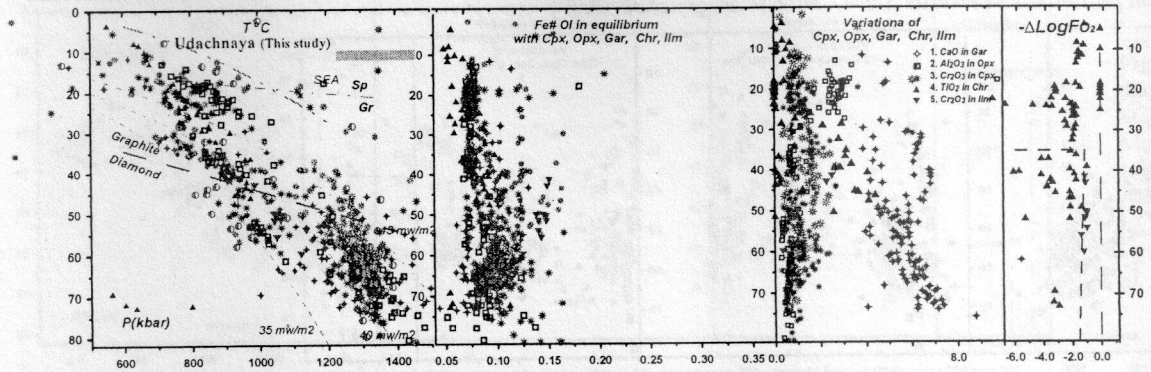

Fig.12. PTXF diagram fore SCLM beneath the Udachnaya pipe, Siberian craton. Our data

In North America the central part of the Slave craton show thick and relatively cold conditions like those found for Jericho and Panda pipe [*Cartigny et al.,* 2009]. But very often they like in Kaapvaal show double PT paths similar to those determined for SCLM beneath Lac de Gras [*Davies et al.,* 2004] (Fig 8). And younger pipes reveal heated conditions to 40 mw/m-2 like those beneath Torrie pipe [*MacKenzie, Canil,* 1999] (Fig.9). The SCLM beneath the Wyoming craton is rather thick and cool but in Mesozoic it is heated and probably reduced [*Hearn et al.,* 1999]

The layered structure of -7-12 horizons correlates with superplume events which is rather similar of the all ancient cratons. The more rough units commonly include 5-7 units like it was determined for Udachnaya pipe showing also deep and cold SCLM using new data set (Fig.12) [*Ashchepkov et al.,* 2010].

Models of the formation of the SCLM are : the nucleation of restite from early mantle it is diapiric, joining of ultra-exhausted blocks of Marianas and island-arc type thickened mantle blocks, the low angle subduction of partially melted plates under superplumes, breaking, cutting of high angle plates and joining to the continental margins. Slabs melting and diapir rising from the depths as deformed peridotites could also increase SCLM. Then fluid/melt flows in the continents margins modified mantle columns. Three traps for the melts: oxidized in- the SCLM base, carbonatite- 45-40 kbar, and water-bearing basaltic- 20-30 kbar were accompanied by the fusions and rising of diapiric at varying SCLM levels. This was accompanied by basification, lithosphere reductions and formation rifts in superplume periods.

Grants RBRF 11-05-00060a;11-05-91060-PICSa

References

1. Ashchepkov I.V., Pokhilenko N.P., Vladykin N.V., Logvinova A.M., Kostrovitsky S.I., Afanasiev V.P., Pokhilenko L.N., , Kuligin S.S., Malygina L.V., Alymova N.V., Khmelnikova O.S., Palessky S.V., Nikolaeva I.V., Karpenko M.A., Stagnitsky Y.B. (2010). Structure and evolution of the lithospheric mantle beneath Siberian craton, thermobarometric study. *Tectonophysics,* v.485, pp.17-41.
2. Aulbach S., Rudnick R. L. McDonough W. F. (2008). Li-Sr-Nd isotope signatures of the plume and cratonic lithospheric mantle beneath the margin of the rifted Tanzanian craton (Labait). *Contrib. Mineral. Petrol.* v.155, pp.79–92
3. Boyd F.R., Pearson D.G., Hoal K.O., Hoal B.G., Nixon P.H., Kingston M.J., Mertzman S.A.(2004) Garnet lherzolites from Louwrensia, Namibia: bulk composition and P/T relations. *Lithos* v.77, pp.473-491
4. Brey, G.P., Kohler, T. (1990). Geothermobarometry in four phase lherzolites II: new thermo-barometers and practical assessment of using thermobarometers. *Journal of Petrology* v.31, pp.1353-1378.
5. Cartigny P., Farquhar J., Thomassot E., Harris J. W., Wing B., Masterson A., McKeegan K., Stachel T. (2009). A mantle origin for Paleoarchean peridotitic diamonds from the Panda kimberlite, Slave Craton: Evidence from 13C-, 15N- and 33,34S-stable isotope systematics. *Lithos.* v.112 S2, 852-864.
6. Davies R.M., Griffin W.L, O'Reilly S.Y.,. Doyle B.J. (2004). Mineral inclusions and geochemical characteristics of microdiamonds from the DO27, A154, A21, A418, DO18, DD17 and Ranch Lake kimberlites at Lac de Gras, Slave Craton, Canada. *Lithos* v. 77, pp.39– 55.
7. Hatton, C.J., Gurney, J.J. (1979). Dimand graphite eclogite from the Roberts Victor Mine. In: F.R. Boyd and H.O.A. Meyer (Editors) *Proceedings of the 2nd International Kimberlite Conference, American Geophysical Union,* v. *2*, pp. 29-36.
8. Harris, J. W. Stachel, T., Léost, I., Brey G. P. (2004). Peridotitic diamonds from Namibia: constraints on the composition and evolution of their mantle source. *Lithos*, v.77, p. 209-223
9. Hearn C. (2004). The Homestead kimberlite, central Montana, USA: mineralogy, xenocrysts, and upper-mantle xenoliths. *Lithos.* v.77, pp. 473– 491
10. Jacob D. E., Bizimis, M, Salters, V. J. M. (2005). Lu–Hf and geochemical systematics of recycled ancient oceanic crust: evidence from Roberts Victor eclogites. *Contrib. Mineral. Petrol.* v.148, pp. 707–720.
11. McGregor, I.D. 1974. The system MgO–Al2O3–SiO2: solubility of Al2O3 in enstatite for spinel and garnet–spinel compositions. *American. Mineralogist* v.59 pp.110–19.
12. MacKenzie J.M., Canil D. (1999). CanilComposition and thermal evolution of cratonic mantle beneath the central Archean Slave Province, NWT, Canada. *Contrib. Mineral. Petrol.* v.134, pp.313 - 324
13. Nimis P., Taylor W. (2000). Single clinopyroxene thermobarometry for garnet peridotites. Part I. Calibration and testing of a Cr-in-Cpx barometer and an enstatite-in-Cpx thermometer. *Contrib. Mineral. Petrol.* v.139, pp.541-554.
14. O'Neill H.St.C, Wood B.J. (1979). An experimental study of Fe-Mg-partitioning between garnet and olivine and its calibration as a geothermometer. *Contrib. Mineral. Petrol.* v.70, pp.59-70
15. O'Neill, H. St. C. & Wall, V. J. (1987). The olivine orthopyroxene-spinel oxygen geobarometer, the nickel precipitation curve, and the oxygen fugacity of the Earth's upper mantle. *Journal of Petrology* v.28, pp. 1169-1191.
16. Richardson, S.H., Pöml P.F., Shirey S.B., Harris J.W. 2009. Age and origin of peridotitic diamonds from Venetia, Limpopo Belt, Kaapvaal–Zimbabwe craton. *Lithos,* v.112S, pp785–792
17. Simon N. S.C., Carlson R.W., Pearson D. G., Davies G. R. (2007). The Origin and Evolution of the Kaapvaal Cratonic Lithospheric Mantle. *Journal Petrology* v.48, pp.589 - 625.
18. Tappert, R., Stachel, T., Harris, J.W., Muehlenbachs, K., Ludwig, T., Brey, G.P. (2005). Diamonds from Jagersfontein (South Africa): messengers from the sublithospheric mantle, *Contrib. Mineral. Petrol.* v. **150**, pp. 505–522.
19. Tsai, H.-M., Meyer, H.O.A. , Moreau, J., Milledge, J. 1979. Mineral inclusions in diamond :, Premier, Jagerfontein and Finsch kimberlites, South Africa, and Williams mine , Tansania. Proceedings of the 2nd International Kimberlite Conference, American Geophysical Union, v.2, pp.16-26.
20. Taylor W.R., Kammerman M., Hamilton R. (1998). New thermometer and oxygen fugacity sensor calibrations for ilmenite and chromium spinel-bearing peridotitic assemblages. 7th International Kimberlite Conference. Extended abstracts. Cape town. pp.891-901
21. Viljoen, K.S., Swash, P.M., Otter, M.L., Schulze, D.J. Lawless, P.J. (1992). Diamondiferous garnet harzburgites from the Finsch kimberlite, Northern Cape, South Africa. *Contrib. Mineral. Petrol.* (1992) v.110, p. 133-138
22. Winterburn, P.A, Harte,B., Gurney J.J., 1990. Peridotite xenoliths from the Jagersfontein kimberlite pipe: I. Primary and primary-

metasomatic mineralogy. *Geochimica et Cosmochimica Acta*, v.54, pp.329-341

Dymshits A.M.[1], Bobrov A.V.[1], Bindi L.[2], Litasov K.D.[3], Shatskiy A.F.[3], Ohtani E.[3], Litvin Yu.A.[4] Synthesis of na-bearing majorte in the system $Mg_3Al_2Si_3O_{12}$ –$Na_2MgSi_5O_{12}$ AT 11-20 GPa: solid solutions and structural features

[1] Geol. dep. MSU; [2] Museo di Storia Naturale, Italy; [3] Univ. Tohoku, Japan; [4] IEM RAS A.Dymshits@gmail.com

Keywords: experiment, mantle, phase transition, Na-bearing majoritic garnet

Currently various ultrahigh-pressure minerals are described as inclusions in diamonds [e.g. Stachel, 2001]. The proof of their truly deep origin often appears problematic because of decompressional structural transformations. Experimental researches available for today, and also complex analysis of the Earth's mantle P–T conditions allow to establish the whole series of the phase transitions and chemical reactions in the conditions of the asthenosphere (> 200 km) and a transition zone (410–660 km). Ultrahigh-pressure minerals, such as MgSiO with ilmenite and perovskite structures, $CaSiO_3$ with perovskite structure, magnesiowustite (ferropericlase), and majoritic garnet. One characteristic feature of this mineral is silicon excess (over 3 pfu) and an isomorphic sodium admixture that allows to carry them to Na-bearing majoritic garnets.

The present experimental researches were aimed on reception of the every possible data about garnet phase $Na_2MgSi_5O_{12}$ (NaMaj): an establishment of pyroxene/garnet phase transition boundaries in *P-T* coordinates, definition of structural features in the pure state and in solid solutions with a pyrope (Prp), and also solubility studying in modeling systems Prp-NaMaj. Experiments were performed in the Tohoku University (Sendai, Japan) at P =11-20 GPa and T= 1500-2100°C on high -pressure Kawai-type apparatus, where cell assemblage with the sample was compressed by eight cubic anvils truncated with triangular faces. Single-crystal shooting of samples was spent with a Bruker-Enraf MACH3 diffractometer using graphite-monochromatized Mo$K\alpha$ radiation. The small crystals were in addition studied with use an Oxford Diffraction Xcalibur 3 diffractometer fitted with a Sapphire 2 CCD detector.

Crystals of a Na-pyroxene and Na-majorite and the fields of their stability were received during experiments at 13-19 GPa [Dymshits et al., 2010]. The phase boundary is described by the equation P (GPa) = 0.0050(2)·T + 7.5(4). Detailed studying of Na-majorite by single-crystal X-ray diffraction has allowed to establish that Na-majorite is tetragonal, space group $I4_1/acd$, with lattice parameters a = 11.3966(6), c = 11.3369(5) Å, V = 1472.5(1) Å^3 [Bindi et al., 2011].

Structures of the garnets with compositions between Na-majorite and pyrope ($NaMaj_{20}$, $NaMaj_{40}$, $NaMaj_{50}$, $NaMaj_{60}$ и $NaMaj_{80}$) were also investigated using a Bruker-Enraf MACH3 single-crystal diffractometer. The results have shown that the increase of NaMaj in starting material leads to gradual reduction of lattice parameter and then to change from cubic to tetragonal at maintenance of NaMaj more than 80 %. It is interesting to notice that similar transformation was observed for pyrope-majorite that is visually presented in Fig. 1 [Parise et al., 1996].

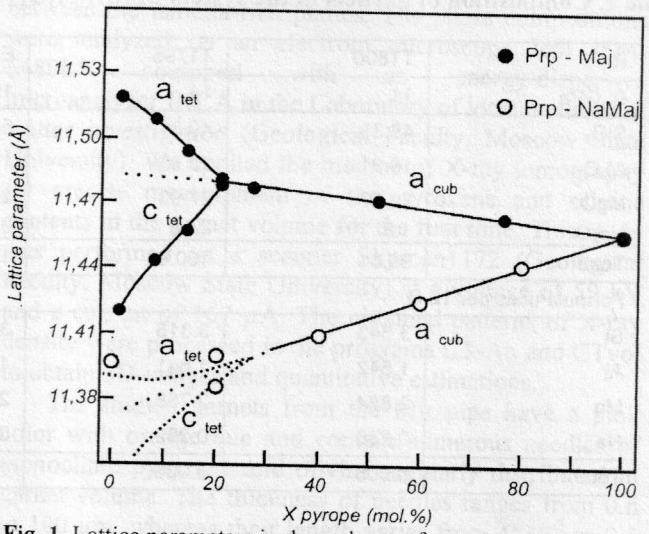

Fig. 1. Lattice parameters in dependence of garnets composition.

Experimental study at 11-20 GPa of the start composition 50 mol.% NaMaj has been spent for demonstrating a tendency of sodium increase in garnet with pressure. Run conditions got out counting upon liquidus crystallization of garnets close to solid that allows receiving the greatest Na concentration. Pyroxene of enstitite-jadeite composition was also found among the run products together with garnet and stishovite at pressures of 11-15 GPa. At pressures over 16 GPa the pyroxene has not been established in run products, and the quantity of stishovite also was the lowest (no more than 5-7%). Garnets with the maximal Na_2O content (>5 wt.%) reached at the assumed solidus of the system and forms subidiomorphic crystals in a small amount of quenched melt (<5%) (Fig. 2). Small phenocrysts (5-10 μm) of sodium rich solid solution with $Na(Mg_xSi_xAl_{1-2x})SiO_4$ ($0<x<0.5$) and MgO content no more 3.8 wt.% together with Grt in are formed with decrease of temperature in run products. This phase, apparently, corresponds $NaAlSiO_4$ (with calcioferrite structure) with a various impurity of $MgAl_2O_4$ component.

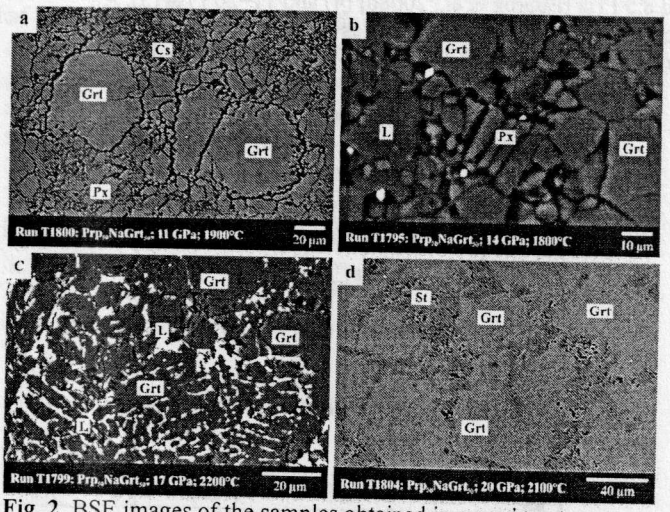

Fig. 2. BSE images of the samples obtained in experiments on the Prp50– Na-majorite50.

As a result of the experiments Na-bearing majorite garnets were synthesized in a wide range of temperatures and pressures, and natural increase of sodium, silicon and,

as consequence, concentration of sodium majorite in garnets with pressure was observed (Fig. 3)

Table 1. Composition of garnets in the system $Mg_3Al_2Si_3O_{12}$– $Na_2MgSi_5O_{12}$

Run	T1800	T1795	ES-243	T1796	T1804
P, GPa	11	14	15	18	20
SiO_2	49.33	49.81	54.86	54.72	56.66
Al_2O_3	19.31	20.93	15.67	17.03	14.57
MgO	28.57	27.93	27.07	24.83	23.52
Na_2O	1.8	2.19	3.72	4.60	5.71
Total	99.01	100.86	101.33	100.00	100.46
Formula units per 12 O					
Si	3.343	3.315	3.630	3.628	3.785
Al	1.542	1.641	1.222	1.330	1.147
Mg	2.884	2.768	2.668	2.452	2.340
Na	0.236	0.282	0.477	0.591	0.739
Total	8.005	8.006	7.997	8.002	8.011

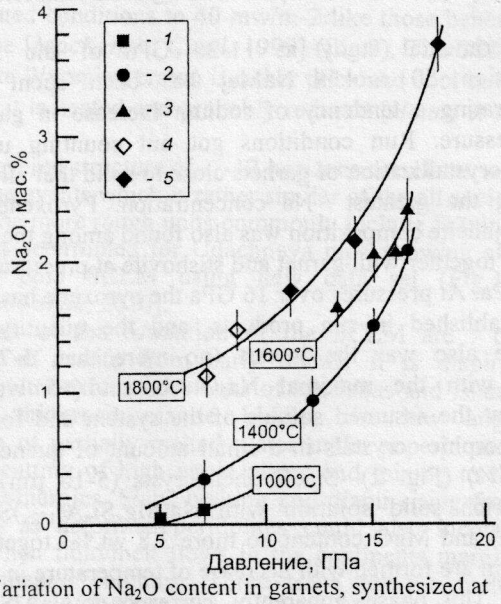

Fig. 3. Variation of Na_2O content in garnets, synthesized at different temperatures and pressures in eclogite system [Okamoto, Maruyama, 1998] (1), MORB [Ono, Yasuda, 1996] (2, 3), modeling system pyrope–$Na_2MgSi_5O_{12}$ (our data) at 7.0 and 8.5 ГПа [Bobrov et al., 2008b] (4) and 11–20 ГПа (5). An accuracy of pressure measurement is indicated by horizontal bars.

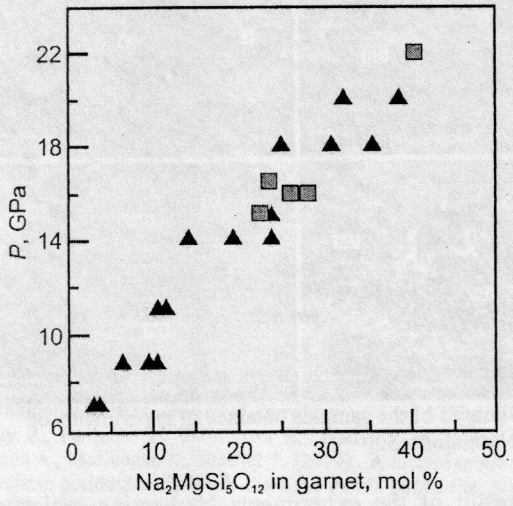

Fig. 4. Solubility of $Na_2MgSi_5O_{12}$ in garnet with pressure in the system Prp_{50}–Na-majorite$_{50}$ (trangles) in comparison to the data [Gasparik, Litvin, 1997] (squares).

Presence of a pyroxene (one more Na-bearing phase) at a number of experiments complicates noted tendency of the garnet liquidus crystallization and leads to change of distribution coefficient of sodium between the garnet and liquid. Nevertheless, from results of experiences follows, that solubility of Na-component in garnet in the studied system at least up to 40 mol%, that is in a good agreement with forsterite-jadeite system (Table 1; Fig. 4) [Gasparik, Litvin, 1997].

Essential solubility of Na-majorite in the pyrope, and also finds of natural garnets with significant concentration of Na (> 1 мас. % Na2O) allows to consider that Na-bearing majoritic garnet can be an important potential sodium concentrator in the lower parts of the upper mantle and transition zone. The successful synthesis of the $Na_2MgSi_5O_{12}$ end-member and its structural characterization is of key importance, because the study of its thermodynamic constants combined with the data of computer modeling provide new constraints on thermobarometry of majorite garnet assemblages.

The study was supported by the Russian Foundation for Basic Research (project nos. 09-05-00027 and 11-05-00401), and grants of the President of Russian Federation for the state support of the young Russian scientists (MD-534.2011.5) and leading scientific schools (NSh-3634.2010.5).

References

1. Stachel T. (2001) Diamonds from the asthenosphere and the transition zone. // *Eur J Mineral. V.* 13. P. 883–892
2. Stachel T., J. Harris, G. Brey, W. Joswig. (2000) Kankan diamonds (Guinea) I: from the lithosphere down to the transition zone. // *Contib Mineral Petrol. V.* 140. P. 1–15
3. Akaogi M., A. Akimoto. (1977) Pyroxene-garnet solid-solution equilibria in the systems $Mg_4Si_4O_{12}$–$Mg_3Al_2Si_3O_{12}$ and $Fe_4Si_4O_{12}$–$Fe_3Al_2Si_3O_{12}$ at high pressures and temperatures // *Phys. Earth. Planet. Inter. V.* 15. P. 90–106.
4. A.V. Bobrov, A.M. Dymshits, Yu.A. Litvin (2009). Conditions of magmatic crystallization of Na-bearing majorite garnets in in the Earth mantle according to experimental and natural data. Geokhimia, N 10, pp. 1011-1026.
5. A.M. Dymshits, A.V. Bobrov, K.D. Litasov, A.F. Shatsky, E. Otani, Yu. A. Litvin (2010). Experimental study of phase transition pyroxene-garnet in the system $Na_2MgSi_5O_{12}$ at pressures 13-20 GPa^ the first synthesis of sodium majorite. Doklady Academii Nauk, V. 434, N 3, pp. 378-381.

6. Bindi L., A.M. Dymshits, A.V. Bobrov, K.D. Litasov, A.F. Shatskiy, E. Ohtani, Yu.A. Litvin (2011) Crystal chemistry of sodium in the Earth's interior: The structure of $Na_2MgSi_5O_{12}$ synthesized at 17.5 GPa and 1700°C // *American Mineralogist, V.* 96, p. 447–450
7. Parise J.B., Y. Wang, G.D. Gwanmesia, J. Zhang, Y. Sinelnikov, J. Chmielowski, D.J. Weidner, R.C. Liebermann (1996). The symmetry of garnets on the pyrope ($Mg_3Al_2Si_3O_{12}$) – majorite ($Mg_4Si_4O_{12}$) join // *Geophys. Research Letters. V.* 23. № 25. P. 3799-3802
8. Gasparik T., Yu.A Litvin. (1997) Stability of $Na_2Mg_2Si_2O_7$ and melting relations in the forsterite-jadeite join at pressures up to 22 GPa // *Eur. J. Mineral. V.* 9. P. 311–326.
9. Okamoto K., S. Maruyama (1998) Multi-anvil re-equilibration experiments of a Dabie Shan ultrahigh-pressure eclogite within the diamond-stability fields // *The Island Arc. V.* 7 . p. 52-69
10. Ono S., A. Yasuda (1996) Compositional change of majoritic garnet in a MORB composition from 7 to 17 GPa and 1400 to 1600 degrees C // *Phys. Earth. Planet. Inter. V.* 96. P. 171–179

Sirotkina E.A., Bobrov A.V., Garanin V.K., Bovkun A.V., Shkurskii B.B., Korost D.V. Exsolution textures in majoritic garnets from the Mir kimberlitic pipe (Yakutia)

Geol. dep. MSU katty.ea@mail.ru

Keywords: majoritic garnet, exsolution textures, upper mantle, X-ray tomography

Majoritic garnets were originally discovered as inclusions in diamonds from the Monastery kimberlitic pipe (South Africa) [Moore, Gurney, 1985], and this find demonstrated that diamonds could contain the matter of asthenosphere and transition zone. Later such garnets were registered in diamonds [Stachel, 2001], mantle xenoliths [Haggerty, Sautter, 1990; Sautter et al., 1991], and rocks of metamorphic complexes [Van Roermund, Drury, 1998] worldwide including Yakutia, Canada, Brazil, China, and Himalaya. They are characterized by the high silicon concentration controlled by incorporation of majoritic component ($Mg_4Si_4O_{12}$) in the mineral structure. In the course of rock uplift to the upper horizons of the Earth, pyroxene lamellae are often exsolved from majoritic garnet. The conditions of primary crystallization of majoritic garnets may be reconstructed by calculation of the concentration of pyroxene lamellae and their composition.

We studied three garnet nodules (Samples 317, 559, and 563) with sizes of >5 mm containing numerous oriented lamellae of pyroxene and olivine from the Mir kimberlitic pipe. Parallel polished sections with a thickness of 0.5-0.8 mm were prepared from garnets, in which relationships between the minerals and their contents were estimated under the microscope in transmitted light. Five-axis universal stage was applied to establish orientations of lamellae and measure the angles between the lamella-rich planes. The phase compositions were analyzed on an electrom microscope Jeol JSM-6480LV equipped with an energy-dispersive microanalyzer INCA in the Laboratory of local methods of matter investigation (Geological Faculty, Moscow State University). We applied the method of X-ray tomography for precise measurement of the pyroxene and olivine contents in the garnet volume for the first time. This study was performed on a scanner Skyscan1172 (Geological Faculty, Moscow State University) at a voltage of 59 kV and a current of 167 μA. The obtained patterns of X-ray density were processed in the programs CT-An and CTvol to obtain 3D-images and quantitative estimations.

The studied garnets from the Mir pipe have a pink color with orange hue and contain numerous needles of monoclinic pyroxene and olivine regularly distributed in garnet volume. The thickness of needles ranges from 0.n to 100 μm, whereas their length varies from $4*10^{-3}$ to 0.5 cm. Acicular inclusions are strictly oriented in garnet by four directions (Fig. 1). Angles between the pairs of crossing needles measured on a five-axis universal stage are 70-71°, which corresponds to the angles between the three-fold axes in the cubic garnet structure. Needles are characterized by polygonal sections and sometimes flattened. Flattening of needles and tables is consistent with rhombododecahedral planes (the angle between closing tables is 60°). Regular orientation of inclusionsand their typical shape allow us to conclude that these needles are the exsolution textures in majoritic garnet. Sample 563 contains only pyroxene lamellae, whereas pyroxene and olivine are observed in Samples 317 and 559 with the strong prevalence of the first mineral.

Microprobe analyses of garnet, clinopyroxene, and olivine are given in Table 1. *Garnets* of all three samples are homogeneous and enriched in pyrope (75-80 mol %). They are characterized by the moderate concentrations of calcium (4.5-5.8 wt % CaO) and relatively low chromium concentrations (up to 0.59 wt % Cr_2O_3), which corresponds to garnet of the lherzolitic paragenesis [Garanin et al., 1991]. The concentrations of Na_2O in garnets are very low (0.06–0.07 wt %). The composition of *clinopyroxenes* corresponds to diopside with small admixtures of hedenbergite and jadeite. Mg# in lamellae practically does not change within the individual sample ranging from 0.90 до 0.94. Pyroxenes are characterized by small admixtures of NiO (0.2-0.3 wt %) and Cr_2O_3 (0.11-0.16 wt %). The composition of *olivines* from Samples 317 and 559 corresponds to forsterite with Mg# of 0.95 in both samples. Olivines are characterized by extremely high nickel concentration (from 1.6 wt % (Sample 559) to 2.79 wt % (Sample 317) NiO). We should note that such high nickel concentrations in olivine are extremely rare.

Table 1. Composition of garnet nodules and intergrowths of pyroxene and olivine from the Mir kimberlitic pipe

	Sample 317				Sample 559				Sample 563		
	Grt	Cpx	Ol	Grt*	Grt	Cpx	Ol	Grt*	Grt	Cpx	Grt*
SiO_2	42.23	54.64	41.40	42.53	42.29	54.32	40.85	42.58	42.66	54.68	43.15
TiO_2	0.02	0.09	0.00	0.03	0.01	0.00	0.00	0.009	0.00	0.04	0.002
Al_2O_3	23.30	1.01	0.12	22.29	23.35	1.80	0.18	22.37	23.61	1.87	22.74
FeO	5.68	1.07	4.42	5.47	5.48	1.09	4.54	5.27	5.45	1.09	5.27
MnO	0.21	0.00	0.00	0.20	0.18	0.00	0.00	0.17	0.24	0.03	0.23
MgO	21.34	17.90	51.20	21.12	22.33	17.26	51.57	22.04	22.21	17.20	22.01

	Sample 317				Sample 559				Sample 563		
	Grt	Cpx	Ol	Grt*	Grt	Cpx	Ol	Grt*	Grt	Cpx	Grt*
CaO	5.72	24.51	0.05	6.44	4.55	23.35	0.00	5.28	4.96	23.46	5.70
Na_2O	0.06	0.47	0.00	0.08	0.06	0.93	0.00	0.09	0.07	1.01	0.11
K_2O	0.00	0.02	0.00	0.001	0.00	0.00	0.00	0.00	0.00	0.00	0.00
NiO	0.00	0.29	2.79	0.013	0.00	0.21	1.64	0.01	0.00	0.20	0.008
Cr_2O_3	0.59	0.11	0.00	0.57	0.43	0.16	0.00	0.42	0.39	0.15	0.38
Total	99.18	100.14	99.98	98.77	98.68	99.15	98.79	98.26	99.59	99.77	99.60
Si	2.993	1.978	1.001	3.018	2.997	1.979	0.996	3.022	2.998	1.980	3.037
Ti	0.001	0.002	0.000	0.001	0.0005	0.000	0.000	0.0005	0.000	0.001	0.000
Al	1.946	0.043	0.003	1.862	1.950	0.077	0.005	1.869	1.955	0.079	1.883
Fe	0.336	0.032	0.089	0.324	0.324	0.033	0.092	0.313	0.320	0.033	0.310
Mn	0.013	0.00	0.000	0.012	0.011	0.000	0.000	0.011	0.014	0.001	0.014
Mg	2.253	0.965	1.846	2.232	2.358	0.937	1.874	2.329	2.325	0.928	2.306
Ca	0.434	0.950	0.001	0.491	0.345	0.911	0.000	0.403	0.373	0.910	0.431
Na	0.008	0.033	0.000	0.011	0.009	0.066	0.000	0.014	0.009	0.071	0.015
K	0.000	0.001	0.000	0.000	0.000	0.000	0.000	0.000	0.000	0.000	0.000
Ni	0.000	0.004	0.054	0.001	0.000	0.003	0.032	0.001	0.000	0.003	0.000
Cr	0.034	0.003	0.000	0.032	0.024	0.005	0.000	0.024	0.022	0.004	0.021
Sum	8.019	4.013	2.996	7.985	8.020	4.012	3.000	7.984	8.018	4.012	8.018

Note. Each analysis is the average of 8-10 analyses in different points. Grt, garnet; Cpx, clinopyroxene; Ol, olivine; Grt*, majoritic garnet, the composition of which is recalculated on the base ox X-ray tomography (95.5% Grt + 4% Cpx + 0.5% Ol.

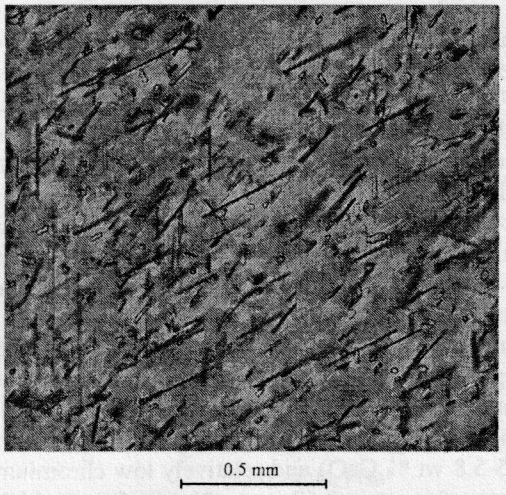

Fig. 1. Exsolution textures in majoritic garnet (Sample 559). Microphotograph is taken in transmitted light.

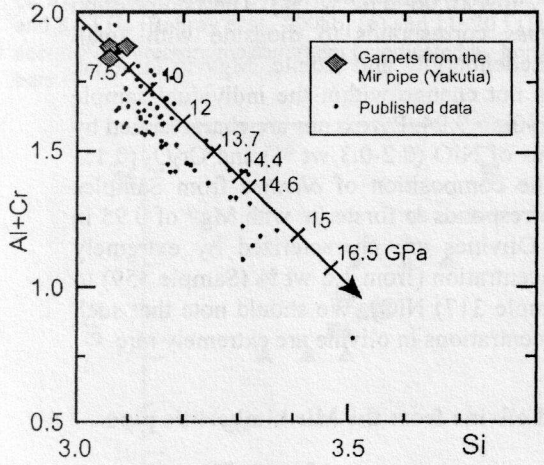

Fig. 2. Compositions of majoritic garnets depending on pressures of their formation, after [Stachel, 2001].

To reconstruct the primary composition of majoritic garnet, we performed the estimation of quantitative content of pyroxene and olivine inclusions in garnet volume using the CT-An software. We used the histogram reflecting the brightness in order to distinguish mineral intergrowths on a set of photographs of parallel sections of majoritic garnet. The detailed 3D analysis of Sample 317 allowed us to establish that garnet contained 9.5 vol % pyroxene and 0.5 vol % olivine. It is necessary to mention that the values obtained characterize the minimal volume concentrations of pyroxene and olivine due to the application of maximally "strict" regime of background removal, as well as impossibility of account for the smallest lamellae. The calculated primary compositions of garnet demonstrate that the concentrations of Si exceed 3 f.u. (Table 1). According to the diagram (Fig. 2), the formation of such garnets occurred at pressures of >7.5 GPa, and subsequently the decrease of pressure resulted in the formation of exsolution textures in them. As this took place, extremely high concentrations of nickel in olivine and nickel admixture in pyroxene provide evidence for the presence of nickel in primary majoritic garnet and high-temperature (~1500°C) crystallization of this mineral [Canil, 1999].

The study was supported by the Russian Foundation for Basic Research (project nos. 09-05-00027 and 11-05-00401), and grants of the President of Russian Federation for the state support of the young Russian scientists (MD-534.2011.5) and leading scientific schools (NSh-3634.2010.5).

References

1. Garanin V.K., Kudryavtseva G.P., Marfunin A.S., Mikhailichenko O.A. (1991) Inclusions in diamonds and diamondiferous rocks, *Moscow: Izd. MSU*, 240 p [in Russian].
2. D. Canil (1999), The Ni-in-garnet geothermometer: calibration at natural abundances, *Contrib. Mineral. Petrol. V. 136. P.* 240-246.
3. S.E. Haggerty, Sautter V. (1990), Ultradeep (>300 km) ultramafic, upper mantle xenoliths, *Science. 248. P.* 993-996.
4. S.E. Haggerty, Sautter V., Field S. (1991) Ultradeep (>300 km) ultramafic xenoliths: petrological evidence from the transition zone, *Science. 252.* 827-830.
5. T. Stachel (2001), Diamonds from the asthenosphere and the transition zone, *Eur. J. Mineral. V. 13. P.* 883-892.
6. H.L.M. Van Roermund, Drury M.R. (1998), Ultra-high pressure (P>6GPa) garnet peridotites in Western Norway: exhumation of mantle rocks from >185 km depth, *Terra Nova.10.* 295-301.